



Research papers

Exploring the food-energy-water nexus in coupled natural-human systems under climate change with a fully integrated agent-based modeling framework

Jiaorui Zhang^a, Y.C. Ethan Yang^{a,*}, Guta W. Abeshu^b, Hongyi Li^b, Fengwei Hung^c, Chung-Yi Lin^d, L. Ruby Leung^e

^a Department of Civil and Environmental Engineering, Lehigh University, Bethlehem, PA, USA

^b Department of Civil and Environmental Engineering, University of Houston, Houston, TX, USA

^c Department of Civil and Environmental Engineering and Earth Sciences, University of Notre Dame, Notre Dame, IN, USA

^d Department of Civil and Environmental Engineering, Virginia Tech, Blacksburg, VA, USA

^e Atmospheric, Climate, and Earth Sciences, Pacific Northwest National Laboratory, Richland, WA, USA

ARTICLE INFO

Keywords:

Socio-ecological systems
Multisector dynamics
Farmers' behavior
Decision scaling

ABSTRACT

Managing water resources to meet increasing energy and food demands while maintaining environmental sustainability under climate change is a major challenge, especially when this nexus occurred in a coupled natural–human system (CNHS), where heterogeneous human activities affect the natural hydrologic cycle and vice versa. The relevant research has been limited by the lack of models that can effectively integrate human dynamics and hydrologic conditions with spatial details to examine co-evolutionary systems. To address this challenge, this paper develops a modeling framework that integrates an agent-based model (ABM; human behavior model) into a large-scale, process-based distributed hydrologic model to simulate human decisions endogenously in the hydrologic cycle. We then apply the Decision Scaling approach, an ex-post scenario analysis method, with our integrated model to study the bidirectional feedback of the CNHS under future changing climate conditions. With the Columbia River Basin (CRB) selected as the case study area, the calibration results show that the integrated model can simultaneously capture the historical irrigated water consumption and streamflow dynamics. Modeling results show that the trade-off between irrigated water consumption, hydropower generation, and streamflow will become more pronounced under hotter and wetter climate conditions at both the entire basin and regional (states and provinces) levels. Special attention should be given to “temperature thresholds” of different regions when the trade-off pattern started. The trade-off results can potentially inform the Columbia River Treaty renegotiation and provide insights for long-term water management policies.

1. Introduction

Managing water resources to meet increasing energy and food demands while preserving the environment is a major challenge. Conventional water resources management studies overlooked the bidirectional feedback (also called co-evolution) between natural and human systems, known as the coupled natural and human systems (CNHS; Giuliani et al., 2016; Testation et al., 2017; Hung et al., 2022; Yang et al., 2020). Consequently, human activities like land use change, infrastructure construction, and water uses were modeled as externally imposed interventions that drove the environmental changes as “one-

way forcing” (Wada et al., 2014; Kahi et al., 2018). This model setting could miss important dynamics in the real CNHS (e.g., the positive, negative, and delayed feedback) that produce unexpected outcomes and affect the sustainability of CNHS (Motesharrei et al., 2014; Liu et al., 2015; Sivapalan et al., 2015; Yoon et al., 2022). Recently, to address this issue, the bidirectional interaction between natural and human systems have been emphasized while using a hydrologic model and a human component to model the interaction mechanism in CNHS.

Two-way coupling, such as file/data exchange between two models, is the most popular method to achieve this interaction in previous studies (Hu et al., 2015; Khan et al., 2017; Lei et al., 2019; Lin et al.,

* Corresponding author.

E-mail address: ye217@lehigh.edu (Y.C.E. Yang).

2022). Human models in these two-way coupled modeling frameworks are simulated by different methods, such as Agent-Based modeling and Social Network Modeling (Castilla-Rho et al., 2015; Kluger et al., 2020; Yoon et al., 2022). For example, Khan et al. (2017) coupled an ABM with the Soil and Water Assessment Tool (SWAT), a process-based semi-distributed hydrologic model, to simulate the impacts of water resources management decision at a watershed scale. Castilla-Rho et al. (2015) coupled nature models (e.g., groundwater model or land-use decision model) into well-developed ABM platforms (e.g., NetLogo) to illustrate potential system responses between natural and human models. Lei et al. (2019) coupled an ABM with the MODFLOW groundwater simulation model to evaluate the outcomes of market-based versus administrative water management strategies. However, the complexity of two-way coupled model can lead to significant computational demands. Reading, processing, and writing the exchanged files can be inefficient and computationally expensive. These limitations can restrict the capability of coupled models to simulate complex systems effectively, particularly in transboundary river basins characterized by intensive human activities (Bhatt et al., 2014; Du et al., 2020). Additionally, ensuring precise data exchange and synchronization between the models to reflect the dynamic interaction can be challenging. For instance, in the absence of an endogenous mechanism to simulate human behaviors, there is a reliance on future external water use data, and the potential for capturing co-evolution between human and natural systems is lost. To accurately simulate the feedback between human and natural system, the tight coupling (fully integrated model) by programming all components (e.g., human and natural systems) within a single modeling framework can significantly reduce data exchange redundancy and is more suitable for complex water system analysis in large river basins. To the best of our knowledge, a fully integrated human and natural system model (e.g., a distributed hydrologic model) is not very common in previous studies. Integrating a human model into the hydrologic framework not only accounts for the dynamic interaction between human actions and water systems but also offers a more nuanced understanding of how individual and collective behaviors can evolve and impact hydrologic processes.

Furthermore, human water decisions have far-reaching implications beyond just the water sector, as water is a vital resource for agriculture, energy production, ecosystem. Therefore, decisions regarding water management can significantly impact other sectors. In recent years, the concept of food, energy, and water (FEW) nexus has been strongly promoted as a global research agenda to analyze Sustainable Development Goals (Leck et al., 2015; Siddiqi et al., 2013). FEW nexus focuses on identifying and analyzing the interconnections among sectors in an effort to facilitate nexus-wide, rather than a single sector, decision-making and promoting more efficient and sustainable resource allocation and use (Bieber et al., 2018; Holtz et al., 2012; Magliocaca, 2020). In addition, management of the FEW nexus also needs to consider spatial scale issues, as decisions made at one scale can potentially have substantial effects on decisions at other scales, which highlights the need for a comprehensive approach to managing the FEW nexus (Reed et al., 2022; Gaddam et al., 2022). However, this multi-scale aspect is commonly underdeveloped in previous FEW studies (Newell et al., 2019). Many studies (e.g., Vogt et al., 2014, Foran, 2015, Kraucunas et al., 2015) prioritized a single spatial scale either from the human system perspective (e.g., a city, a state or a country) or from the natural system perspective (e.g., a catchment, a watershed or a river basin). While some studies have employed multi-regional input-output (MRIO) analysis to explore multi-scale issues in the FEW nexus (Nawab et al., 2019; Siderius et al., 2020), this method may struggle to fully capture the dynamic interactions between FEW sectors, particularly when they span multiple regions with varying policies and environmental conditions. Additionally, the static assumption of MRIO analysis limits its ability to evaluate future scenarios and anticipate long-term sustainability challenges. This limitation is particularly pertinent in the FEW nexus, where understanding the implications of future climate changes

is vital. The acute and long-term climate stresses can lead to infrastructure or socioeconomic shocks such as outages, supply disruptions at different sectors (e.g., energy or water). Moreover, shocks at smaller scales can have cascading effects that are transmitted to a larger scale through tipping points that trigger critical, propagating changes (Holdschlag et al., 2013; Reed et al., 2022). Thus, a new approach capable of discerning the dynamic of the nexus, incorporating various scales and levels of analysis, recognizing the trade-offs (defined as improvement in one sector but deterioration in another) and synergies between them, and promoting communication and coordination across scales and sectors is needed.

Motivated by the aforementioned knowledge gaps, this study aims to advance our understanding of the co-evolution mechanism in CNHS and how this mechanism influences the FEW nexus under climate change impacts. The objectives of this paper are (1) developing a distributed modeling framework that integrates an agent-based model which simulates spatially distributed human behaviors (i.e., irrigation decisions), into a process-based distributed hydrologic model to mimic human systems endogenously in the hydrologic cycle, (2) evaluating the interaction of different sectors (food, energy, water, and environment sector represented through ecosystem-related like seasonal flow fraction) by using the modeling results from our integrated model to potentially inform relevant policies under various climate change scenarios at different scales (i.e., basin-wide, state/province or subbasin level). The modeling framework is applied to the Columbia River Basin (CRB) that crosses Canada and the US as a case study for illustration. The distributed modeling framework can address the computational challenge and data exchange issue via the modularized ABM inside an existing hydrologic model. In addition, the shift from exogenous to endogenous irrigation decision, which transitions from an externally coupled model to a dynamically simulated one, allows us to evaluate future FEW nexus without the need for external water use data. Moreover, the setup of the distributed modeling framework can naturally output results from regional (defined as states and provinces in this paper) to basin scales and identify where potential trade-offs of water use might arise under various climate change scenarios.

The remainder of this paper is structured as follows. Section 2 describes the case study area. Section 3 shows the detailed integrated modeling framework and the numerical experiment designs. The results are shown in Section 4, followed by the discussion in Section 5. Finally, we present our conclusions in Section 6.

2. Case study – The Columbia river basin

The Columbia River is North America's fourth-largest river by flow volume. It drains an area of 668,000 km² and covers portions of seven States (Washington, Oregon, Idaho, Montana, Wyoming, Nevada, and Utah) in the US and the Canadian Province of British Columbia (Fig. 1). Water resources of the Columbia River Basin (CRB) are heavily managed to satisfy multiple (often competing) objectives including hydropower generation, flood control, agricultural withdrawals, instream flow requirements for fish, and recreational needs (Hamlet et al., 2010; Rajagopalan et al., 2018). Hydropower created by dams along the Columbia River and its tributaries provides more than 70 % of the Pacific Northwest's energy needs and account for 40 % of the US hydropower production (U.S. Energy Information Administration, 2014). However, the ability to manage the dams for maximum power production has been influenced by the need to increase river flows in the spring and summer to protect the salmon population. Furthermore, these in-streams demands compete with out-of-stream water uses such as irrigation. Irrigated agriculture has a significant impact on the CRB's water resources, and agricultural withdrawal is the largest consumptive water use of Columbia River with around 14,200 km² of irrigated area in the CRB (Rajagopalan et al., 2018). FEW nexus is particularly sensitive to climate change in the CRB. The basin's natural hydrology, which relies heavily on winter snow accumulation and melt, has been disrupted due to rising

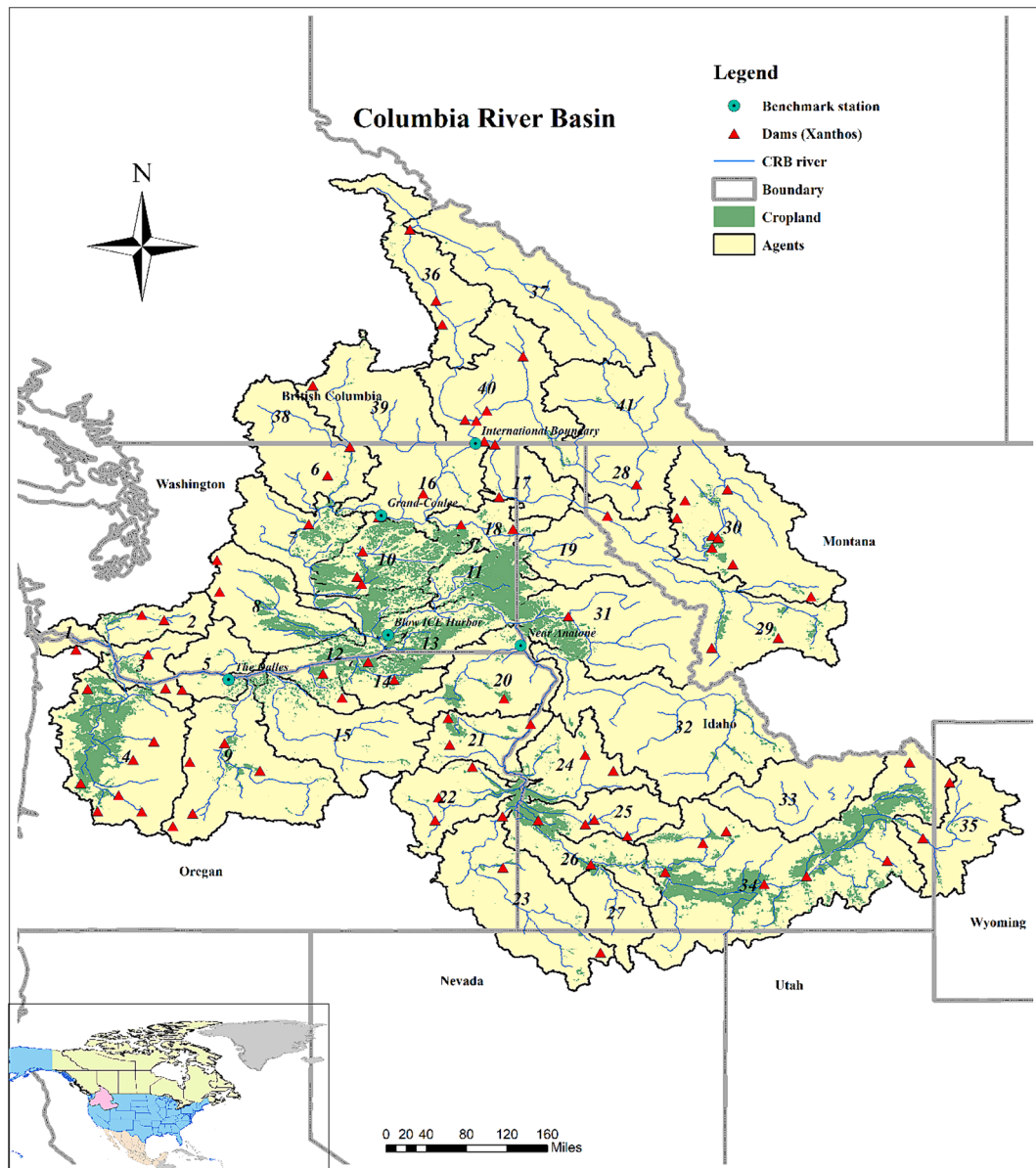


Fig. 1. The boundary, cropland, and major dams of Columbia River Basin modeled in this study. The blue circles are the gauge stations used for calibration and validation purpose. The numbers indicate the locations of agents we defined in the Columbia River Basin. (For interpretation of the references to color in this figure legend, the reader is referred to the web version of this article.)

temperatures (Mantua et al., 2010; Payne et al., 2004). This has resulted in decreased snowpack, altered streamflow timing, increased peak streamflow, and higher water temperatures (Chang et al., 2013; Luce et al., 2014), as well as subsequent effects such as power deficits during the summer, reduced salmon survival, and increased various species of salmonids' susceptibility to disease and predators (Chegwidden et al., 2016; Crozier, 2015; Sauter et al., 2001).

In this study, the CRB, which features a typical CNHS, will be used as the case study to test the proposed integrated modeling framework. In particular, we will quantify the FEW nexus under different climate scenarios and evaluate how these changes will affect food, energy, water and ecosystem sectors at the entire basin and different regions of the CRB.

3. Methodology

3.1. The hydrologic model - Xanthos

Xanthos is a global hydrologic model developed to estimate water availability at monthly scale (Li et al., 2017; Vernon et al., 2019). Utilizing a distributed approach, this Python-based tool operates at a spatial resolution of 0.5 degrees (<https://github.com/JGCRI/xanthos>), providing granular insights into monthly water dynamics. The enhanced version of Xanthos integrates features accounting for local water withdrawals and reservoir operations, underlining its adeptness at merging both natural processes and human influences in water management (Abeshu et al., 2023). Its modular design grants users the flexibility to customize configurations of its main components, including potential evapotranspiration estimation method, runoff generation model, routing model, and subsequent data post-processing. We use Xanthos for our modeling framework because: 1) Xanthos's capability to explicitly represent in-stream water infrastructures, such as dams and reservoirs,

Table 1
Calibrated parameters for Xanthos.

| Parameter | Description | Range |
|------------|--|----------|
| a | Propensity of runoff to occur before the soil is fully saturated | [0,1] |
| b^* | Upper limit on the sum of evapotranspiration and soil moisture storage | [0,4000] |
| c | Degree of recharge to groundwater | [0,1] |
| d | Release rate of groundwater to baseflow | [0,1] |
| m | Snowmelt coefficient | [0,1] |
| η | Velocity adjustment coefficient | [0,10] |
| ϵ | Reservoir capacity reduction factor | [0.5,1] |

*The unit for this parameter is mm.

ensures a comprehensive understanding of human influence on streamflow dynamics, and 2) The inherent modular architecture of Xanthos facilitates its seamless integration with other models, thereby broadening its applicability in multifaceted research environments.

The core of Xanthos includes three modules: potential evapotranspiration (PET), runoff generation, and river routing. The monthly PET can be calculated using different methods including the Penman-Monteith, Hargreaves-Samani or Thornthwaite method (Note: Penman-Monteith, which is widely recognized for its accuracy in various climates, is applied in this study, and this method considers factors such as temperature, humidity, wind speed, and solar radiation to provide a comprehensive estimation of PET). The runoff generation module (ABCD hydrologic model) uses monthly PET, precipitation (P) and maximum/minimum air temperature as inputs and defines five parameters “ a ”, “ b ”, “ c ”, “ d ” and “ m ” that reflect hydrologic regime characteristics (Liu et al., 2018; Sankarasubramanian & Vogel, 2003; Thomas, 1981) to simulate monthly water fluxes (e.g., runoff, groundwater recharge) and pools (e.g., soil moisture, groundwater) in the grid cell. The river routing module includes a cell-to-cell river routing scheme adopted from the modified river transport model (MRTM), which uses a linear advection formula to calculate the outflow leaving the grid cell to its downstream neighboring (Zhou et al., 2015). Abeshu et al. (2023) improved Xanthos by adding a channel velocity adjustment coefficient, η , in MRTM to account for the uncertainties in the channel velocity field and introducing a water management module that represents local human water uses and reservoir activities. Monthly local human water uses for different purposes such as domestic, electricity, and irrigation are exogenous inputs and simply subtracted from the total runoff and the remainder of the runoff is discharged into the channels and routed downstream through MRTM. Reservoir operation is described based on the main purpose (e.g., irrigation, hydropower, flood control) of each reservoir. For irrigation and flood-control reservoirs, the reservoir capacity reduction factor, ϵ , was applied to the final release function of the reservoirs. For hydropower reservoirs, the release policies are derived using stochastic dynamic programming. The underlying equations and detailed algorithms are described in Abeshu et al. (2023). All the gridded global monthly climatic data, including precipitation, maximum temperature, and minimum temperature, were sourced from the WATer and global CHange (WATCH; Weedon et al., 2011) dataset. We incorporated global reservoir data sourced from the Global Reservoir and Dam (GRanD) dataset (Lehner et al., 2011). The monthly water use data for various sectors, presented at a spatial resolution of 0.5 degrees, were obtained from Huang et al. (2018).

To apply the global-scale Xanthos in our case study area, CRB, and

integrate with an ABM, three modifications are needed: (1) tailoring the Xanthos’s geographical focus to specifically include only the CRB; (2) changing the river routing units for smaller subbasins; (3) converting human water use component from exogenous to endogenous. For the first modification, we only model the 336 grid cells that cover the CRB domain out of the global land grid, which comprises 67,420 cells, to reduce computational time. For the second modification, we delineate 41 different subbasins inside the CRB following the Fish and Wildlife Program from Northwest Power and Conservation Council (NPCC, 2005, shown in Fig. 1). Each subbasin will have different calibrated values for the Xanthos parameters listed in Table 1. The third modification is the main scientific contribution of this study. The human water use component (Huang et al., 2018) is originally treated as exogenous inputs in Xanthos. However, this setting limits us from evaluating the co-evolution of human and water systems. To overcome this limitation, we integrate an ABM (details in the next two sections) into Xanthos and calculate the human water use component endogenously.

3.2. The human behavior model - ABM

In this study, we only focus on irrigation decisions by farmers in the ABM, given that agriculture significantly impacts water consumption within the CRB. While we currently emphasize agricultural water use, the scope for incorporating other water users, such as those for hydropower and municipal needs, remains open for future research endeavors. The CRB was segmented into 41 distinct subbasins in this study. We define farmers or farmers groups inside these subbasins as agents. And for the simplicity purpose, the current model only sets up one agent in each subbasin. An agent’s water usage is the aggregated irrigation water consumption in the subbasin. Every year, agents need to develop their cropping plans for the coming year and their decision-making process may be influenced by economic (e.g., crop price), social (e.g., labor), and environmental (e.g., nutrient management) considerations. Studies also suggested that past climate and hydrologic conditions can influence farmers’ water use decisions (e.g., Eisele et al., 2021; Lizumi et al., 2015). For simplicity, this study only focuses the discussion on irrigated water consumption by encapsulating the consideration into two variables, agent’s past experience and future water availability. Given that most farms are primarily focused on profitability (English et al., 2002; Khanal et al., 2021), we assume agents are profit-driven, and their goals are to increase crop production by maximizing irrigated water consumption. It is important to note that this assumption should be used with caution, as it may not fully capture the complexities and varied motivations in agricultural practices (Featherstone et al.,

Table 2
Calibrated parameters for ABM.

| Parameter | Description | Range |
|------------|---|--------|
| α^0 | Farmer’s initial prior knowledge about next year is a wet year | (0,20] |
| β^0 | Farmer’s initial prior knowledge about next year is a dry year | (0,20] |
| e | Cost factor for water consumption | [0,1] |
| γ | The percentage of total water availability farmers think they can use | [0,1] |
| f | The ratio of next year precipitation farmers think they cannot use | [0,1] |

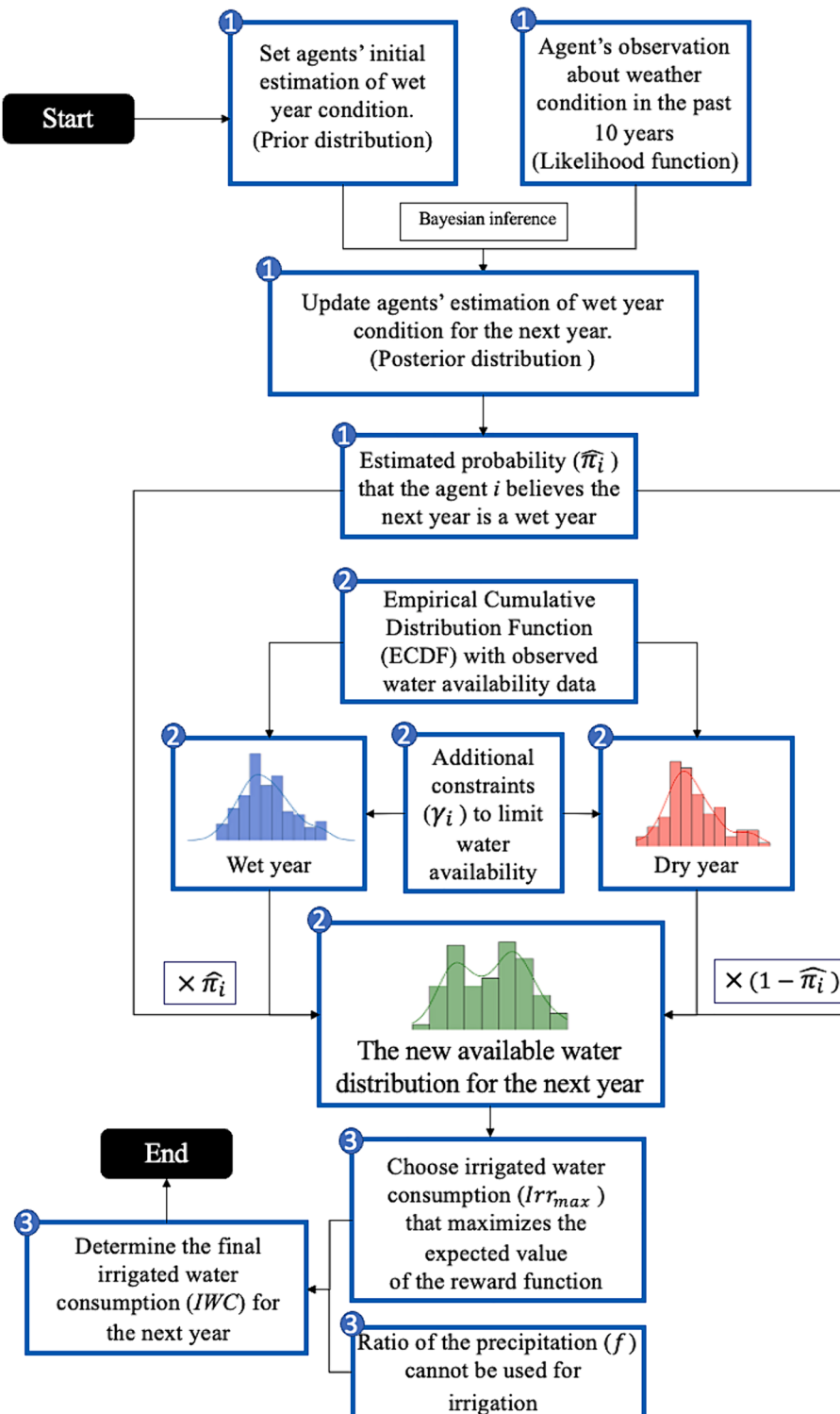


Fig. 2. Agents' decision-making process at the annual timescale. Numbered circles represent three steps. Step 1: agents estimate the probability that they believe the next year is a wet year. Step 2: agents estimate water availability conditions for the following year based on Step 1. Step 3: agents decide how much water they need for irrigation in the next year driven by the economic value of their crop production.

1995; Salimonu et al., 2007; Alderman et al., 2007; Olarinde et al., 2008). The current study does not explicitly simulate agricultural activities (e.g., crop selection, double cropping, and crop area) and market mechanisms (e.g., crop price) but use irrigated water consumption as a proxy of crop production. More detailed discussions about our ABM limitations are provided in Section 5.2.

In our ABM, when water is scarce, agents may consider reducing

their water consumption in response to the potential water shortage. Every agent has five parameters describing their decision-making process that need to be calibrated (Table 2). In our design, agents' decision-making involves three steps as indicated by the numbered circles in Fig. 2. The first two steps are the Bayesian inference for estimating the probability of future water availability, and the third step is an optimization process that utilizes the probabilistic information to maximize

irrigated water consumption. The standard Overview, Design concepts, and Details + Decision (ODD + D) description (Müller et al., 2013) for the ABM (Table S1) is provided in the [Supplementary Materials](#).

In step 1, agents estimate the probability that they believe the next year is a wet year (i.e., water availability larger than the long-term average). This estimation draws on literatures that show farmers' capacity to recognize and integrate historical climate trends (e.g., wet or dry condition) into their decision-making process (Gadgil et al., 2002; Moyo et al., 2012), and Harrell et al. (2022) indicated that the irrigation pattern is different in dry year and wet year in the CRB. The water availability observed by each agent depends on its location within the river network. Headwater agents' water availability is defined as the total runoff generated inside the subbasin. Non-headwater agents' water availability is calculated as the sum of the runoff within their subbasins and the streamflow from all upstream subbasins. We apply the Bayesian inference approach in Eq. (1) to update agents' wet year beliefs of next year. Eq. (1) shows a generic expression of Bayesian inference.

$$P(\pi|x)\propto f(x|\pi) \times P(\pi) \quad (1)$$

where π is a random variable representing the probability of the next year being a wet year and it depends on x which is the observed number of wet years in the past n years ($n = 10$ years in the case study). $P(\pi)$ is the agents' prior distribution of π . The likelihood function $f(x|\pi)$ is the probability that x is observed. $P(\pi|x)$ is the posterior distribution of π after taking into account the observed x . In our simulation, this resulting posterior in the current year will be the prior in the next year, which is an iterative process to update the agents' beliefs. Moreover, the design of this updating process emphasizes the agent's recent experience, which represents their short-term memory of recent climate anomalies (n years). Practically, a wet or dry year will be applied to the updating process for n times, and thus the recent experience will carry a higher weight through the updating process. We use the Beta distribution (Eq. (2)) to describe the agents' beliefs in the probability of wet year since it is particularly useful for modeling probabilities that are based on limited or subjective information, like personal beliefs or experiences (O'Hagan, 1998).

$$P(\pi_i) \sim \text{Beta}(\alpha_i^0, \beta_i^0) \quad (2)$$

where $P(\pi_i)$ is the probability distribution of agent i 's beliefs that the next year is a wet year. α_i^0 and β_i^0 are initial shape parameters of the Beta distribution. Following the setting by Ng et al. (2011), weather-related variables (to describe the occurrences of climatic events) can be assumed to be binomially distributed. We use this assumption for the likelihood function in Eq. (3) to describe the occurrences of wet years:

$$f(x_i|\pi_i) \sim \text{Bin}(n, \pi_i) \quad (3)$$

where x_i represents the number of wet years that agent i observes within a n -year period which means the agents only consider their observation in the past n years and experience beyond that has little influence on their water availability perception. The posterior distribution is also a Beta distribution (Eq. (4)) with updated shape parameters α'_i and β'_i . We can apply Eq. (5) and (6) to update the posterior distribution because Beta distribution is conjugate to Binomial distribution (Press, 2002).

$$P(\pi_i|x_i) \sim \text{Beta}(\alpha'_i, \beta'_i) \quad (4)$$

$$\alpha'_i = \alpha_i^0 + x_i \quad (5)$$

$$\beta'_i = \beta_i^0 + n - x_i \quad (6)$$

In our study, α_i^0 and β_i^0 (shown in Table 2) represent the agents' prior expectation (a degree of belief) about the relative likelihood of the next year being a wet year versus dry year, respectively. For example, when α_i^0 is larger than β_i^0 , it means the agent starts with a belief that the next

year is more likely to be wet than dry. We obtained the posterior distribution of π_i and would still like to have a single estimate $\hat{\pi}_i$ for π_i . The posterior mean and posterior mode are commonly used as Bayesian estimate $\hat{\pi}_i$ for π_i . In this study, we choose the posterior mean (Eq. (7)) as estimator, which is the probability that agents i believes the next year being a wet year:

$$\hat{\pi}_i = \frac{\alpha'_i}{\alpha'_i + \beta'_i} \quad (7)$$

One issue in the Beta distribution updating for human behaviors is that α'_i and β'_i values increase when the number of observations accumulates (Eqs. (5) and (6)). This phenomenon will dilute the information provided by new observations. For example, if α_i^0 and β_i^0 are both "1", the prior mean is $\bar{\pi}_0 = 0.5$, and we observed two wet years in the recent 10 years ($x_i = 2$). The updated posterior mean is $\hat{\pi}_i = 0.25$, which is a decrease of 0.25. Whereas if α_i^0 and β_i^0 are both "20", the prior mean is still $\bar{\pi}_0 = 0.5$. But the two wet-year observations will only update the posterior mean $\hat{\pi}_i = 0.44$ (a decrease of 0.06). This example shows that the new observation's effect on the posterior depends on the sum of α_i^0 and β_i^0 and will decrease over time as more observations are received. Essentially, it means that the agents remember all the events, each event affects the agents' decision-making equally regardless of when it happened, and the effects of individual events decrease as the agents accrue more data. However, this contradicts the scientific understanding of how the human brain works. Literature has pointed out that human memory is limited, and the newer events have a stronger effect on humans' perception (Khalvati et al., 2019). To address this issue, we assume that the sum of α_i^0 and β_i^0 represents an agent's memory length and fix the memory length throughout the simulation (i.e., $\alpha_i^0 + \beta_i^0 = \text{constant}$). We applied a constant decay rate σ_i ($0 \leq \sigma_i \leq 1$) to the prior in the Bayesian updating process to account for the memory fading effects, as shown in Eqs. (8) and (9):

$$\alpha'_i = \sigma_i \times (\alpha_i^0 + x_i) \quad (8)$$

$$\beta'_i = \sigma_i \times [\beta_i^0 + (n - x_i)] \quad (9)$$

Eqs. (8) and (9) are plugged into Eq. (7) to obtain the estimated probability that agent i believes the next year being a wet year. The decay rate and modified process give a higher weight to recent observations compared to the distant past. Individual agents' memory length can differ from agent to agent. Hence, we constructed Eq. (10) to determine the agents' decay rate σ_i based on the observation size (n ; $n = 10$ in this case study) and initial α_i^0 and β_i^0 , which is determined by model calibration.

$$\sigma_i = \frac{\alpha_i^0 + \beta_i^0}{\alpha_i^0 + \beta_i^0 + n} \quad (10)$$

The decay rate design ensures the shape parameters sum of the posterior ($\alpha'_i + \beta'_i$) equals to that of the prior ($\alpha_i^0 + \beta_i^0$).

In step 2, agents estimate water availability conditions for the following year based on their beliefs of the next year is a wet year from step 1 ($\hat{\pi}_i$). In cognitive science, mixture distributions are utilized to model how different cognitive processes jointly influence the behavior on task-based activities (Cole and Bauer, 2016; Nicenboim et al., 2021). By using a mixture distribution in step 2, farmers can incorporate different water availability conditions into their planning and decision-making processes. We used W_t and D_t to represent an agent i 's beliefs of the water availability distribution of the wet and dry years, which are constructed by the Empirical Cumulative Distribution Function (ECDF) with observation. The ECDF is constructed from the historical records of water availability for wet and dry years. The mixture water availability distribution of agent i can be calculated by Eq. (11).

$$ND_{i,t+1} = \hat{\pi}_i \times (W_{i,t} \times \gamma_i) + (1 - \hat{\pi}_i) \times (D_{i,t} \times \gamma_i) \quad (11)$$

where $ND_{i,t+1}$ is the water availability distribution that agent i thinks it can use in the next year, and the parameter $\gamma \in (0, 1)$ represents the additional constraints that prevent the agents from accessing all the available water such as water rights and conveyance losses. $\hat{\pi}_i$ is the probability that agent i 's beliefs the next year is a wet year, and $(1 - \hat{\pi}_i)$ represents the probability that agent i 's beliefs the next year is a dry year. For example, let us consider an agent i who estimates the probability of the upcoming year being wet from step 1 is 0.3. Consequently, the belief in the next year being dry is $1 - 0.3 = 0.7$. The agent then allocates weights based on these probabilities to respective water availability distributions for wet ($W_{i,t}$) and dry ($D_{i,t}$) years. Additionally, the agent takes into account external constraints, $\gamma_i = 0.6$, which limit the utilization of available water resources. Therefore, the anticipated water availability distribution for next year's irrigation, $ND_{i,t+1}$, is calculated as $ND_{i,t+1} = 0.18 \times W_{i,t} + 0.42 \times D_{i,t}$. Eq. (11) represents the weighted sum of water availability under both wet and dry conditions, adjusted for the external constraints. To enhance readability and facilitate comprehension of the analysis, we will omit indices i and t in the subsequent equations.

In step 3, agents will decide how much water they need for the irrigation in the next year driven by the economic value of their crop production while considering the risk of water shortage. For simplicity, detailed simulation of agricultural activities and market dynamics are not considered. Instead, irrigated water consumption is employed as an indicative measure of crop production. An agent's reward function (R) is defined in Eq. (12) where a penalty term ($e \times Irr$) is introduced to farmers' production function to represent the economic costs (e.g., the sunk costs of fertilizers).

$$R = \begin{cases} Irr - e \times Irr, & \text{if } ND > Irr \\ ND - e \times Irr, & \text{if } ND \leq Irr \end{cases} \quad (12)$$

where Irr is irrigated water consumption decision for the next year. e is a cost factor, and the range is from 0 to 1. ND is obtained from the new water availability distribution from Eq. (11). This function exhibits asymmetry. In years with ample water ($ND > Irr$), the function reflects the agent's expected profit. Conversely, during water-scarce years ($ND \leq Irr$), the overestimation of water availability introduces a sunk cost, adversely impacting the agent's overall profitability. An agent's objective is to choose an Irr_{max} to achieve a better expected value of the reward (Eq. (13)).

$$E[R] = \int_0^{Irr} (ND - e \times Irr)f(ND)dND + \int_{Irr}^{+\infty} (Irr - e \times Irr)f(ND)dND \quad (13)$$

Reorganizing Eq. (13), we can get:

$$E[R] = (Irr - e \times Irr) + \int_0^{Irr} (ND - Irr)f(ND)dND \quad (14)$$

$$Irr_{max} = \operatorname{argmax} E[R] \quad (15)$$

where $f(ND)$ is the probability corresponding to the water availability distribution of ND .

Furthermore, we assume the next year's precipitation forecast will affect the agent's irrigated water consumption and they can obtain the next year's precipitation forecast from public information sources. In this study, the precipitation information is from WATer and global CHange (WATCH; Weedon et al., 2011). Part of the direct precipitation (*Precip*) can be used for crop water needs depending on its timing and volume. If rain falls outside of the cropping season, the water volume does not contribute to satisfy crop water needs. Therefore, an agent's actual irrigated water consumption (*IWC*) is calculated by subtracting a fraction of precipitation from Irr_{max} (Eq. (15)) where $f \in (0, 1)$ represents the ratio of rainfall that cannot be used for irrigation.

$$IWC = Irr_{max} - Precip \times f \quad (16)$$

3.3. ABM and Xanthos integration

In this study, ABM and Xanthos are integrated at the source code level, i.e., ABM is integrated into the relevant module of Xanthos. The internal data exchanged between Xanthos and ABM are (1) agents' water use (irrigated water consumption from ABM), and (2) hydrologic condition (streamflow from Xanthos) at the annual time step. Note that we assume the subsequent year's precipitation forecast influences the agent's irrigated water consumption, rendering the precipitation data external to the ABM. The integrated model is simulated at a monthly time scale to capture the seasonal irrigated water consumption patterns and how that affects FEW nexus. The workflow of the integrated model is shown in Fig. 3. Xanthos is initialized to compute the natural hydrologic processes, including potential evapotranspiration, surface runoff, and streamflow at the monthly scale. The resulting streamflow is first aggregated to annual scale and fed to ABM to calculate the agent's annual irrigated water consumption. After determining the agent's total irrigated water consumption for the coming year using the algorithm in

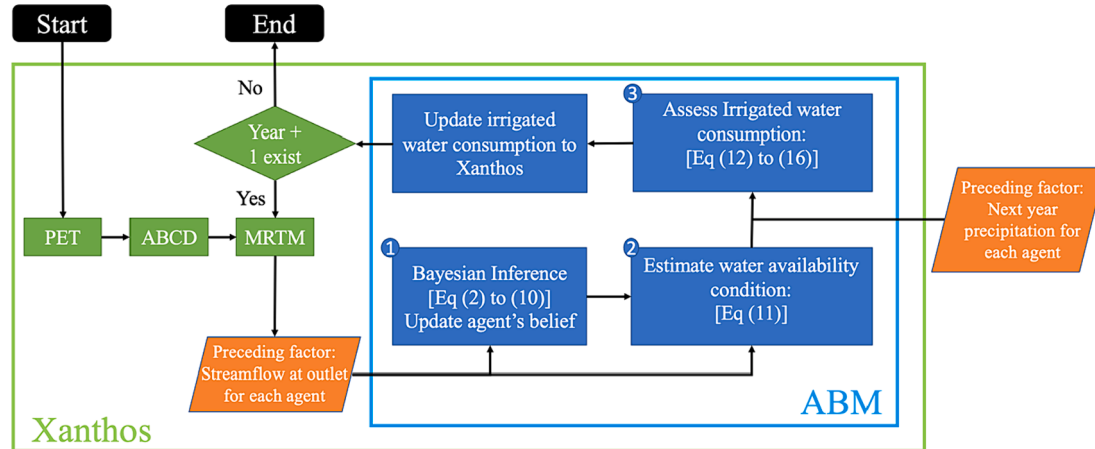


Fig. 3. The workflow of integrated ABM-Xanthos. The green line represents the original Xanthos, and the solid green boxes of "PET", "ABCD", and "MRTM" represent the core modules of Xanthos. The blue line is the ABM, and the blue boxes summarize agents' behavior rules, which are detailed in Fig. 2. (For interpretation of the references to color in this figure legend, the reader is referred to the web version of this article.)

Fig. 2, we use the historical pattern of monthly irrigated water uses data to allocate annual irrigated water consumption back into the monthly scale. Finally, the monthly total water uses of each subbasin (irrigation, domestic, cooling of thermal power plants, etc.), which are the input data for Xanthos, are calculated by adding the monthly irrigated water consumption with the monthly water uses in other sectors from Huang et al. (2018). Note that in our current integrated model, the focus is on irrigated water consumption. Therefore, we assume that the monthly water uses in other sectors will remain the same as the historical averaged values.

We use the historical streamflow data from five US Geological Survey gauge stations (blue circles in Fig. 1) and irrigation water uses from Huang et al. (2018) to evaluate the performances of the integrated ABM-Xanthos model. The calibration period is from 1971 to 1990 and the validation period is from 1991 to 2001. The Kling-Gupta efficiency (KGE, Gupta et al., 2009) and its modified version (KGE', Kling et al., 2012), with a range from negative infinity to "1" (i.e., a perfect model), are used as the main indicators to judge model performances.

3.4. Numerical experiment designs

To quantify the highly uncertain future climate change effects on irrigated water consumption, hydropower generation, and streamflow at different spatial scales, we apply the decision-scaling framework as proposed by Brown et al. (2012). This ex-post scenario analysis method focuses on identifying acceptable system performance in a broad range of future climate conditions rather than focusing on projections of future climate that are subject to uncertainties in various climate modeling and downscaling approaches. To evaluate a wider range of climate changes beyond what is projected to the basin according to the full ensemble of General Circulation Model (GCM) projections, the monthly historical precipitation (P) and temperature (T) record (1972–2001) are resampled and perturbed to construct 30-year monthly time series of P and T representing plausible future climate changes. Specifically, temperature increases range from 0 °C to 7 °C with 1 °C increments added to the 30-year resampled temperature monthly data, and precipitation changes ranging from -30 % to +30 % with 10 % intervals are used as a multiplier for the precipitation monthly data. These changes in P and T, yielding 7 precipitation and 8 temperature conditions respectively, lead to 56 representations of climate changes. The 56 representations are used as inputs to the integrated model. We repeat the procedure of resampling the historic record 30 times (with each of the 30 samples referred to as a single “trial”) to address the internal climate variability. Each trial represents one plausible climate condition for the next 30 years. The 56 climate change representations along with each trial of the resampled 30-year climate bring the total number of simulations involved in this study to 1680 (30 × 56). The GCM projections under Coupled Model Intercomparison Project 5 (CMIP 5) scenarios: Representative Concentration Pathway (RCP) 2.6, 4.5, 6.0 and 8.5 were used to inform the likelihood of future climate conditions. The RCPs describe four different scenarios based on different assumptions about population, economic growth, energy consumption and sources and land use over this century (Van Vuuren et al., 2011). A list of all GCMs employed in this study, under each RCP, has been provided in the Supplemental Materials (Table S3).

We applied the concept of elasticity to quantify the nexus between irrigated water consumption (the proxy of the food sector), hydropower generation (the proxy of the energy sector), and streamflow (the proxy of the water and environment sector). Elasticity is a measure of a variable's sensitivity to a change in another variable (Schaake, 1990; San-karasubramanian et al., 2001). In this study, we evaluate the irrigated water consumption impact on streamflow and hydropower generation at different spatial scales under the 56 climate change representations. The irrigated water consumption (IWC) elasticity of streamflow (Q), ε_{IQ} , and IWC elasticity of hydropower generation (HP), ε_{IH} , are calculated by Eqs. (17) and (18).

$$\varepsilon_{IQ} = \frac{\overline{Q}_{future,j} - \overline{Q}_{base}}{\overline{Q}_{base}} / \frac{\overline{IWC}_{future,j} - \overline{IWC}_{base}}{\overline{IWC}_{base}} \quad (17)$$

$$\varepsilon_{IH} = \frac{\overline{HP}_{future,j} - \overline{HP}_{base}}{\overline{HP}_{base}} / \frac{\overline{IWC}_{future,j} - \overline{IWC}_{base}}{\overline{IWC}_{base}} \quad (18)$$

where $\overline{Q}_{future,j}$, $\overline{HP}_{future,j}$, and $\overline{IWC}_{future,j}$ are average annual streamflow, hydropower generation and irrigated water consumption under climate change scenario j . \overline{Q}_{base} , \overline{HP}_{base} , and \overline{IWC}_{base} are average annual streamflow, hydropower generation, and irrigated water consumption from the baseline scenario (0° C change in temperature and 0 % change in precipitation). In our study, ε_{IQ} and ε_{IH} can fall into one of four types: (1) elasticity value > 1 (no trade-off) means that IWC is elastic and changes in Q (or HP) is more than proportionally getting impacted by a variation in IWC, (2) elasticity value < -1 (trade-off exist) means that IWC is elastic and the decrease or increase in Q (or HP) is more than proportionally getting impacted by an increase or decrease in IWC, (3) $-1 <$ elasticity value < 1 means that IWC is inelastic and Q or HP is relatively insensitive to IWC, (4) elasticity = 1 or = -1 means that IWC is unit elastic and changes in IWC result in an equal change in Q and HP. For a detailed illustration of the methodology applied to calculate elasticity across different sectors under varying climate conditions, refer to Fig. S1 in the *Supplementary Materials*. This figure provides a schematic representation of the analytical process, using IWC and HP as exemplars, it visually presents the calculation of IWC elasticity of HP under various climate scenarios.

4. Results

4.1. Calibration and validation of the integrated model

Fig. 4 shows that the overall performances of Xanthos' streamflow results at five stations are close to or greater than 0.5, which represent reasonable calibration and validation results. An exception was noted for the Grand Coulee station, with a lower KGE and KGE' value (0.47). Due to the real-world complex reservoir operation rules for multiple purposes of irrigation, hydroelectric generation, and flood management, the current reservoir component in Xanthos cannot capture 100 % of the reservoir releases of the Grand Coulee dam. However, this bias does not significantly affect streamflow further downstream. Therefore, the calibration and validation results of Xanthos are acceptable for our purpose. **Fig. 5** shows the calibrated and validated results for agents with the largest irrigated water consumptions. Most KGE and KGE' values are higher than 0.5 which indicate our model can generally capture the pattern and trend of historical irrigated water consumption. The results of other agents with smaller irrigated water consumption are in the *Supplementary Materials* (Fig. S2). Although the modeled irrigated water consumptions are “less accurate” compared to the observation data, these endogenously calculated irrigated water consumptions allow us to explore the bidirectional interactions between the human and natural systems and how those interactions affect the FEW nexuses, as long as the trend and pattern of human decisions can be reasonably captured. Furthermore, this change will allow us to further apply this integrated model for future FEW nexus evaluations while no future water uses data is needed. This is the major difference of our integrated model compared the models used in previous studies (Voisin et al., 2013; Wada et al., 2014; Kahi et al., 2018).

4.2. Multiple sectors result at the basin scale

The impact of climate change (i.e., different precipitation and tem-

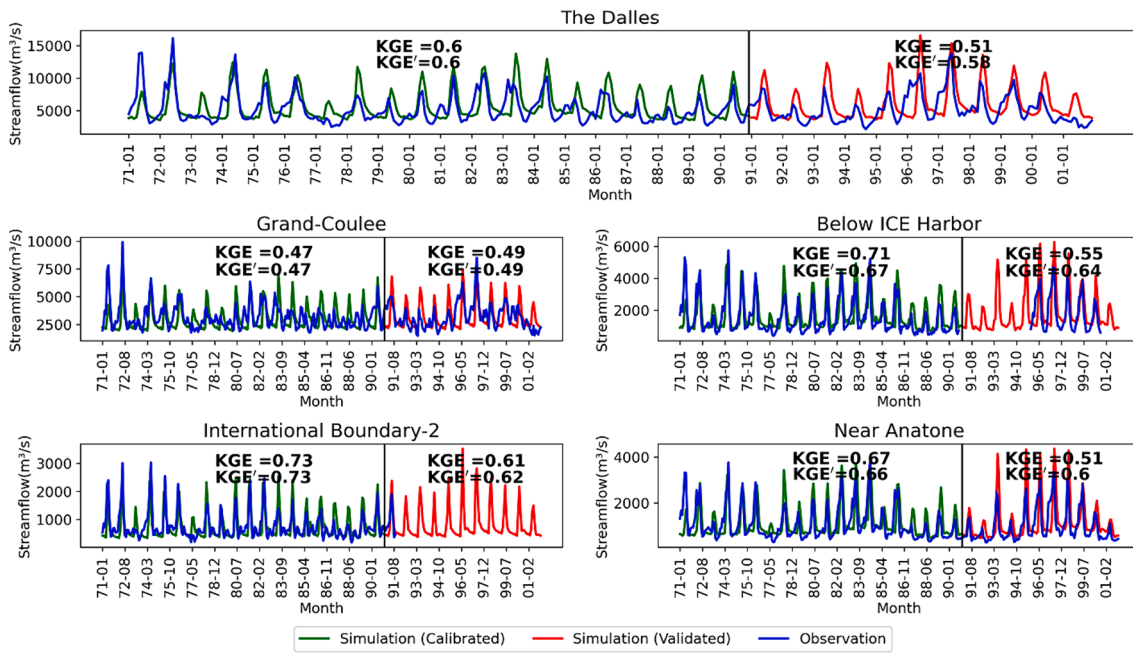


Fig. 4. The calibration and validation results of five streamflow stations in the CRB: The Dalles, Grand-Coulee, Below Ice Harbor, International Boundary-2, and Near Anatone. Blue lines are for observed streamflow data. Green lines and red lines represent calibrated and validated results, respectively. (For interpretation of the references to color in this figure legend, the reader is referred to the web version of this article.)

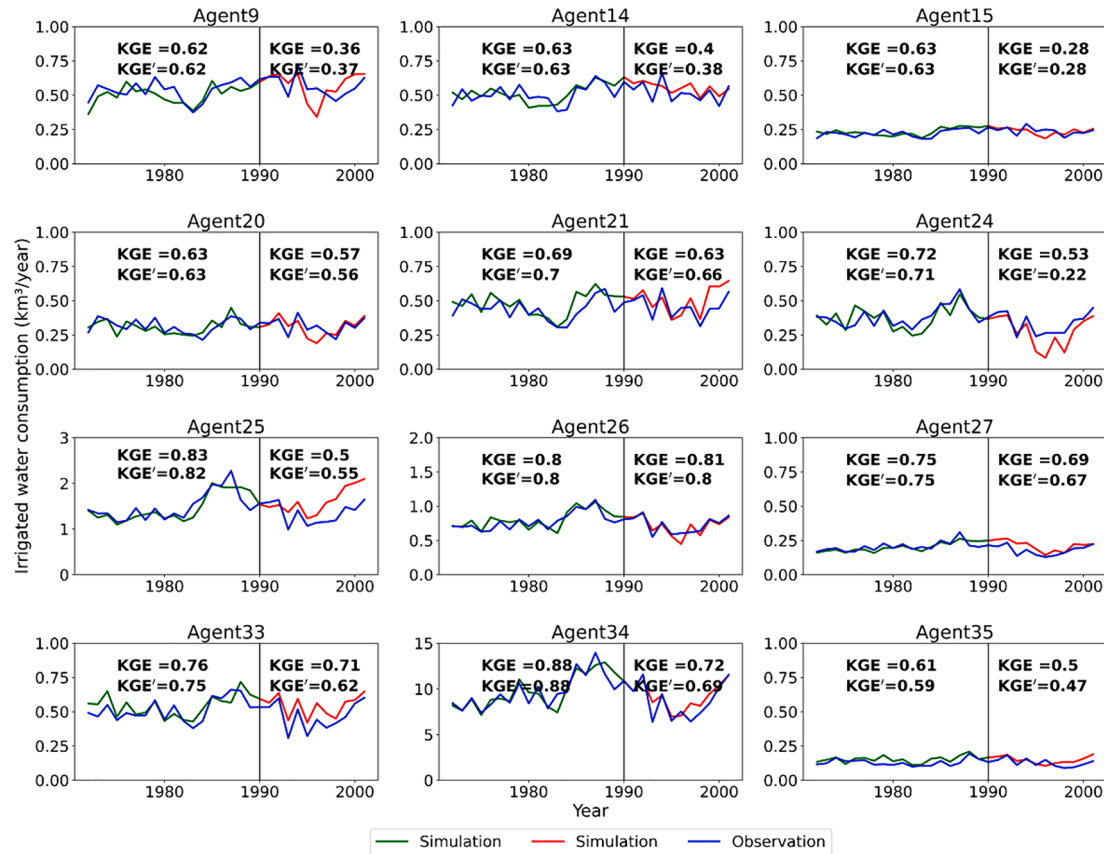


Fig. 5. The calibration and validation results of example agents in the CRB. Blue lines are for observed irrigated water consumption. Green lines and red lines represent calibrated and validated results, respectively. (For interpretation of the references to color in this figure legend, the reader is referred to the web version of this article.)

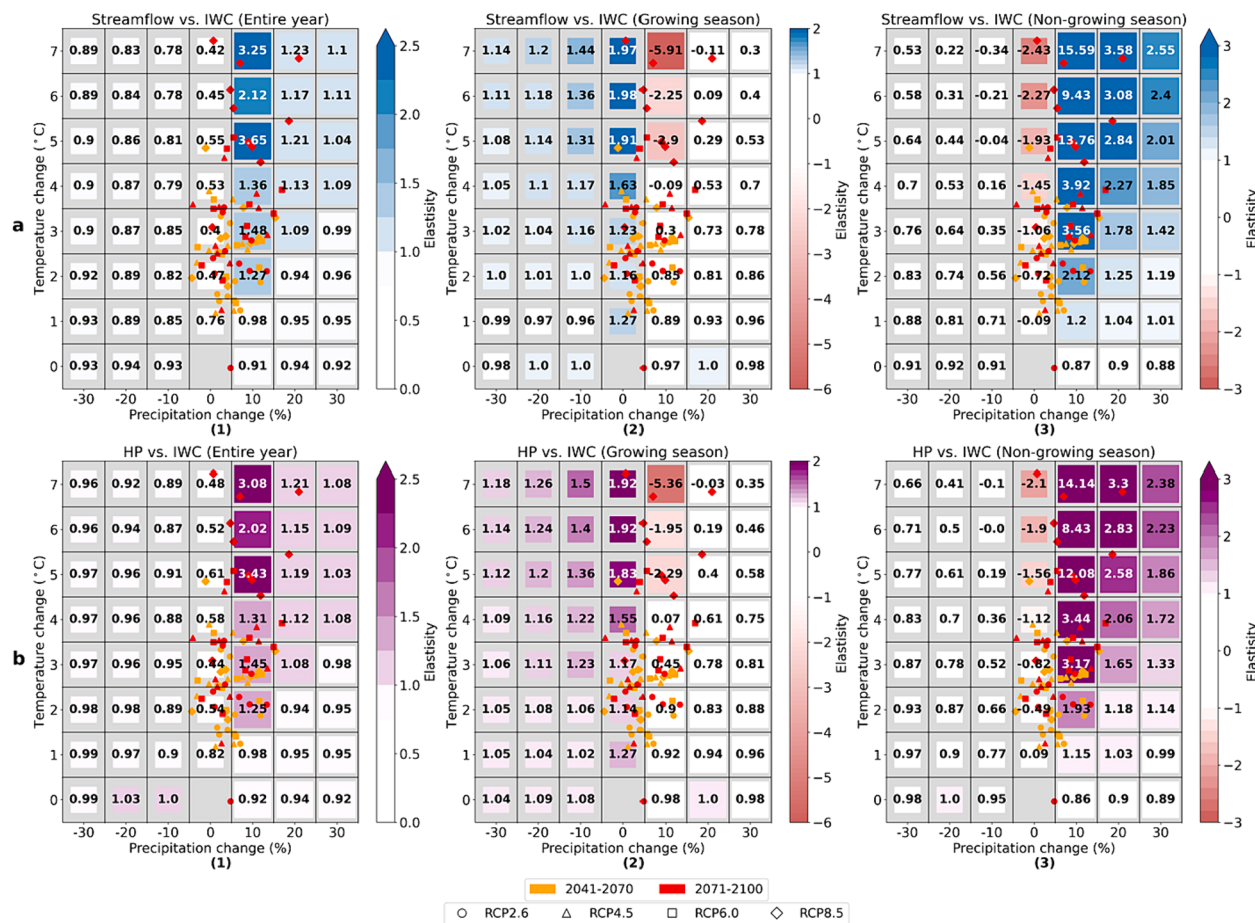


Fig. 6. Climate response surfaces for elasticity on basin-wide irrigated water consumption, streamflow, and hydropower generation. Superimposed points show GCM projections obtained from the CMIP5 ensemble (orange color represents climate projections: 2041–2070; red color represents climate projections: 2071–2100). Circles, triangles, squares, and diamonds represent RCP 2.6, 4.5, 6.0 and 8.5 respectively. IWC and HP represent Irrigated water consumption and hydropower generation, respectively. The smaller size of the colored grid indicates the average annual irrigated water consumption is lower than the baseline level. (For interpretation of the references to color in this figure legend, the reader is referred to the web version of this article.)

perature) on annual irrigated water consumption (km^3), annual hydropower generation (GW) and annual streamflow (m^3/s) are shown in the Supplementary Materials (Fig. S3). However, these results do not explicitly demonstrate the trade-offs among these sectors. Therefore, Fig. 6 uses heat maps of climate response surface (Brown et al., 2012), which are two-dimensional diagrams depicting the patterns of related model outputs under different combinations of temperature and precipitation changes, to illustrate the impacts of climate change on basin scale elasticity between different sectors. Fig. 6a and b show the average annual irrigated water consumption elasticity of the average annual streamflow (ε_{IQ}) and the average annual irrigated water consumption elasticity of the average annual hydropower generation (ε_{IH}), respectively. The distinct columns (1), (2), and (3) indicate different periods of calculation: the entire year, the growing season (April to September), and the non-growing season (October to March). Different color scales represent positive or negative elasticity values. The white color indicates elasticity value between “1” and “-1.” The smaller size of the colored grid indicates the average annual irrigated water consumption is lower than the baseline level. The baseline elasticity values of these climate response surfaces are for 0°C temperature change and 0% precipitation change and their corresponding grids in Fig. 6 are shown as blank. All the y-axis and x-axis of heat maps indicate the temperature changes and precipitation changes, respectively. Furthermore, downscaled GCM projections of CMIP 5 scenarios: RCP 2.6, 4.5, 6.0 and 8.5 (different dots in Fig. 6) from different years (2041–2070 in orange and 2071–2100 in red) are superimposed on these climate response surfaces to visualize

the likelihood of the future climate change range. The results show that all GCMs project some warming ranging from 1°C to 5°C in 2041–2070 and from 1°C to 7°C in 2070–2100. Projected changes in mean annual precipitation range from 5% decrease to about 16% increase in 2041–2070, and from about 5% decrease to 23% increase in 2070–2100. Overall, the result from the CMIP5 ensemble suggests a warmer and wetter future in the CRB.

All elasticity values in Figs. 6a-1 and b-1 are positive, indicating no trade-off between streamflow and IWC or HP and IWC when we calculate elasticity for the entire year. In addition, these two figures show higher positive elasticity values under increased precipitation change ($10\%, 20\%, 30\%$) combined with warmer temperature (from 3°C to 7°C), especially when precipitation increase of 10% is combined with a temperature increase greater than 4°C . Given that this is the climate change range suggested by GCMs, a minor increase/decrease in IWC can result in sensitive streamflow and hydropower increase/decrease in the most likely future. Figs. 6a-2 and b-2 show the results of the growing season. We observe positive values of ε_{IQ} and ε_{IH} under dry scenarios (precipitation change from 0% to -30%) which means no trade-off. The positive values mean a decrease in streamflow and HP will be more sensitive to a decrease in IWC under these dry conditions. One possible explanation is that the water availability is drastically diminished under these conditions and observed by our agents to reduce their IWC. Despite this, the dry conditions continue to have a significant impact on streamflow and hydropower generation. On the other hand, we also observe negative values of ε_{IQ} and ε_{IH} when precipitation

increases by just 10 % combined with a temperature change greater than 4 °C which mean there are trade-offs in these climate conditions. This result means that both streamflow and HP can significantly fall below the baseline levels under these conditions while IWC would remain above baseline levels. These findings have important implications for water resource management. For example, implementing strategies to reduce IWC and increase water use efficiency, such as encouraging the use of more efficient irrigation technologies in the growing season will be very helpful in mitigating these trade-offs. When precipitation increases more than 10 %, these trade-off patterns disappear since more water become available in the basin. Figs. 6a-3 and b-3 show the results of the non-growing season. There are positive elasticity values of ε_{IQ} and ε_{IH} under wet scenarios (precipitation change from 10 % to 30 % and temperature change from 1 °C to 7 °C) which, again, means no trade-off. These results mean that significant increases in streamflow and hydropower generation are more sensitive to IWC increase under these wet conditions. This is the opposite reason compared to what we have in the growing season. Since water availability is drastically increased under wet conditions, while our agents observed this pattern and slightly increase their IWC, the increase in streamflow and hydropower are more substantial than IWC increases. More importantly, the non-growing season results show that there is a trade-off between streamflow and IWC or HP and IWC when no change in precipitation is combined with a temperature change greater than 3 °C, which means that the IWC decrease below baseline levels (i.e., smaller color grids) while both streamflow and HP increase during these scenarios. One explanation is the accelerated snowmelt in mountainous regions due to rising temperatures. This early snowmelt augments streamflow during the non-growing season, leading to a potential increase in hydropower generation. Detailed results elucidating the shift in peak flow due to the early snowmelt are available in the Supplementary Materials (Figs. S4 and S5). Despite the increasing water availability in the non-growing season, the overall water availability throughout the entire year experiences a decline due to increasing evapotranspiration caused by increasing temperature. Since agents in the current model use annual water availability and precipitation to determine IWC, consequently their annual decisions lead to a slight decrease in IWC during the non-growing season and result in this trade-off.

GCMs result from 2041 to 2100 in Fig. 6 also reveals important insights regarding the timing of potential trade-offs between the food, water, and energy sectors. Specifically, the projected climate conditions during 2041–2070 indicate that trade-offs between sectors are not very clear in this time period (i.e., no red grid overlaps with orange dots). This outcome implies that the existing water infrastructure or regulatory policies might be able to address the water demand conflicts in this timeframe. However, the likely future climate during 2071–2100, especially for RCP6.0 (red square) and RCP8.5 (red diamond), may result in a clear trade-off between sectors (i.e., red grids overlap with red

dots). To mitigate these potential water demand conflicts, the existing regulation plans might need some modification, which could involve revising the allocation strategies and exploring innovative approaches to balance the needs of various sectors.

Alternatively, we can also demonstrate the trade-off between different sectors in the Pareto front format. For example, Fig. 7 uses the x-axis to show hydropower generation change and the y-axis to show irrigation water consumption change. We use different colors to represent different temperature increases and different symbols to represent different precipitation changes. The plots have four different zones and only the scenarios located in Zones I and IV indicate trade-off (i.e., one sector goes up, another goes down). For example, trade-off exists in Zone I when IWC increases, and HP decreases in the growing season. We also observed trade-off in Zone IV when IWC decreases, and HP increases in the non-growing season. For the entire year, no future scenarios result in any trade-off between IWC and HP.

4.3. Multiple sectors result at the regional scale (IWC vs. HP)

Section 4.2 provides the basin-wide relationship between irrigation, streamflow, and hydropower generation. In this section, we present results aggregated from subbasins level (i.e., agent) for four U.S. states: Washington (WA), Oregon (OR), Idaho (ID), and Montana (MT), and one province in Canadian: British Columbia (BC) inside the CRB to show the spatial heterogeneity among different regions (i.e., multiple scales). We highlight the changes in IWC and HP in these areas as demonstrations. Similar to Fig. 6, we also use heat maps of climate response surface to show the impacts of climate change on the regional scale elasticity between IWC and HP based on our integrated model. Fig. 8a to e represent the average annual irrigated water consumption elasticity of the average annual hydropower generation (ε_{IH}) for WA, OR, ID, MT and BC, respectively. All other settings are similar to Fig. 6.

Looking at the results for the entire year (Fig. 8a-1 to e-1), all of the elasticity values for WA and OR are positive, indicating that these two states located in the downstream portion of CRB will not experience a trade-off between IWC and HP due to climate change. On the other hand, when precipitation increases by 10 % and temperature increase by more than 2 °C, upstream states (ID and MT) and Canada (BC) will see some trade-offs (i.e., negative elasticity values) between IWC and HP. We also observe different “temperature thresholds” that might trigger these trade-offs. For MT and BC where the absolute amount of IWC is smaller than other parts of the basin, a 2 to 3 °C temperature increase seems to be the starting point of the IWC and HP trade-off. For ID where the absolute amount of IWC is among the largest in the basin, temperature increase needs to reach 5 °C for us to observe the trade-offs. These trade-offs are the results of the interaction between IWC, Irr_{max} , and precipitation described in Eq. (16) (Section 3.2). With a 10 % increase in precipitation, Irr_{max} also increases due to increased streamflow but with a

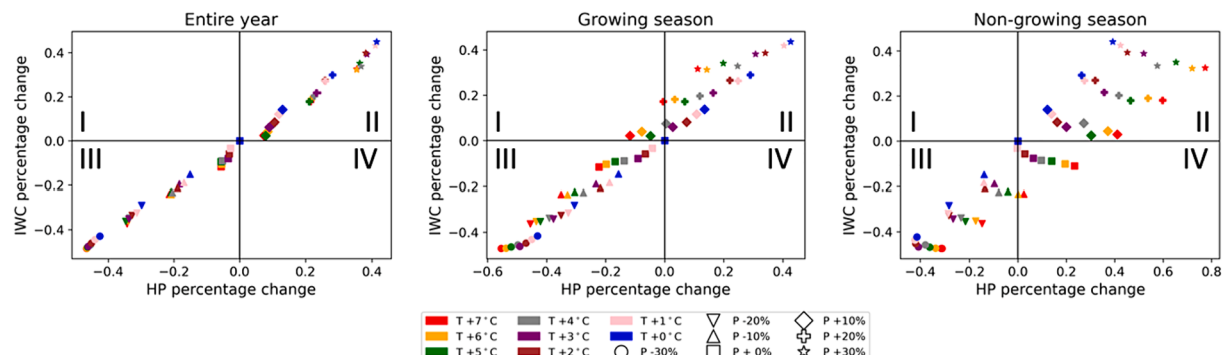


Fig. 7. Pareto Front depicting the trade-offs between percentage changes in irrigated water consumption (IWC) and hydropower generation (HP) under varied climate change scenarios. Different colors represent different temperature increases, while distinct symbols denote variations in precipitation changes. (For interpretation of the references to color in this figure legend, the reader is referred to the web version of this article.)

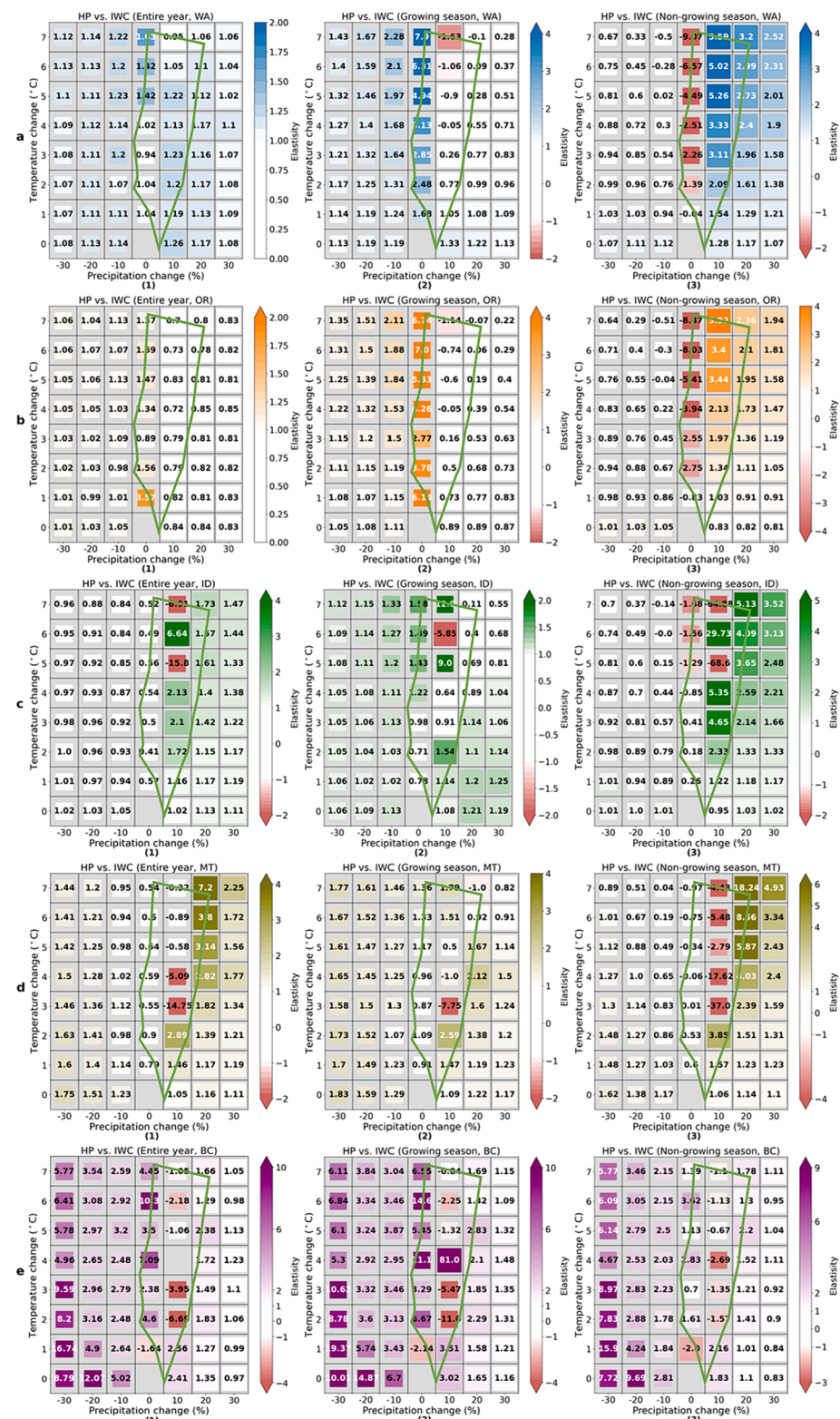


Fig. 8. Climate response surfaces for elasticity on regional irrigated water consumption (IWC) and hydropower generation (HP). WA, OR, ID, MT and BC represent the States of Washington, Oregon, Idaho, and Montana, and British Columbia in Canada, respectively. The green polygon is the boundary of GCM projections to visualize the possible range of climate change. The smaller size of the colored grid indicates the average annual irrigated water consumption is lower than the baseline level. (For interpretation of the references to color in this figure legend, the reader is referred to the web version of this article.)

smaller magnitude. When this happens, agents will assume more crops can become rain-fed, resulting in a slight decrease in their IWC decisions. When precipitation increase more than 10 %, more streamflow becomes available, and agents will increase their IWC. Therefore, the

trade-offs disappear. The distinct “temperature thresholds” between the upstream states and the province may be due to the sensitivity of snowmelt changes caused by increasing temperature (both in terms of timing and volume), subsequently affecting water availability and Irr_{max} .

Fig. 8a-2 to e-2 show the results of the growing season and **Fig. 8a-3 to e-3** show the results of the non-growing season. The trade-off patterns show up in different locations and different climate conditions. For the downstream states (WA and OR), a clear seasonal pattern can be observed. Trade-offs happen only under the extreme temperature increase condition (7°C) and with a 10 % precipitation increase in the growing season, but in the non-growing season, trade-offs can happen when temperature increases by more than 2°C . In the growing season, falling HP and increasing (or the same) IWC is the main reason for trade-offs. Conversely, in the non-growing season, the driving factors are reversed. For upstream states and the province, each part of the CRB seems to have its own pattern. In ID, we also observe the seasonal difference in trade-offs, but the pattern is not linear. The opposite pattern shows up when temperature increases by 6°C and precipitation increases by 10 %. The main reason for this result is the internal climate variability. We derived a higher average precipitation in the 6°C scenario compared to the 5°C and 7°C scenarios in our resampling process. Consequently, this results in a greater average water availability increase, leading to a more substantial rise in IWC. Furthermore, the “temperature threshold” for trade-off patterns to be observable is 5 to 6°C which is higher than that in downstream states. In MT, most trade-offs occur in the non-growing season starting at 3°C temperature increase. We do observe an anomaly under 3°C temperature increase and 10 % precipitation increase condition in the growing season. However, since the absolute amount of IWC is very small in MT, this result can be caused by the sensitivity of the modeling results or again the effect of internal climate variability. Finally, we do not observe a clear seasonal difference in trade-offs in BC. The “temperature threshold” of trade-offs starts at 2°C temperature increase for both growing and non-growing seasons. However, since there are not many agricultural activities in this part of BC, the absolute amounts of these trade-offs are not severe.

These results indicate that 1) balancing the timing of crop production and hydropower generation will become more challenging under climate change in different parts of CRB; 2) special attention should be given to the “temperature thresholds” of different regions when trade-off pattern starts to be observed; and 3) region-specific water management policy will be needed for upstream and downstream states to address

these trade-offs under climate change.

4.4. Multiple sectors result at the subbasin scale (IWC vs. Streamflow for fish)

Climate change could also affect culturally and economically important aquatic species, such as Chinook salmon (*Oncorhynchus tshawytscha*) in the CRB (Columbia River Inter-Tribal Fish Commission, 2013; Williams and Hardison, 2006). These species populations have been in decline due to degraded ecosystems caused by reduced snowpack and altered rainfall and runoff pattern (in addition to damming and operation). The interpretation of treaty-guaranteed water rights in light of changing conditions will become a contentious and pressing issue as competition for water intensifies (Dalton et al., 2013).

Our integrated model can provide some insights about the trade-offs between streamflow for fish and IWC under multiple climate change scenarios for different subbasins in the CRB. We choose two subbasins (i.e., agents) located on Yakama tribal ceded lands (Agent 7) and Umatilla tribal ceded lands (Agent 12) for demonstration purposes. We use Seasonal Flow Fraction (SFF, Stewart et al., 2005), which is defined as the ratio of the spring-summer (April-July) flow volume to the water year flow volume, to represent environmental flow requirements for ecosystem. The spring-summer period is crucial to the salmon life cycle (Independent Scientific Group, 2000), as water is required for juvenile and adult salmon habitat and migration. **Fig. 9** is the heat map of climate response surface to show the effects of climate change on the average annual IWC elasticity of average annual SFF for these two agents. All other settings are similar to **Figs. 6 and 8**.

Figs. 9-1 and 9-2 reveal that there is no trade-off between SFF and IWC for Agent 7 and Agent 12 under no precipitation change scenarios. Notably, Agent 12 shows higher positive elasticity values as temperature increases from 4°C to 7°C , indicating that a decrease in SFF will be more significantly impacted by a decrease in IWC. This might be due to the fact that the total average annual IWC in Agent 12 is much higher than Agent 7. Moreover, both Agent 7 and Agent 12 will experience a trade-off between IWC and SFF when precipitation increases by 10 % alongside temperature increments exceeding 5°C . Particularly, Agent 12 will

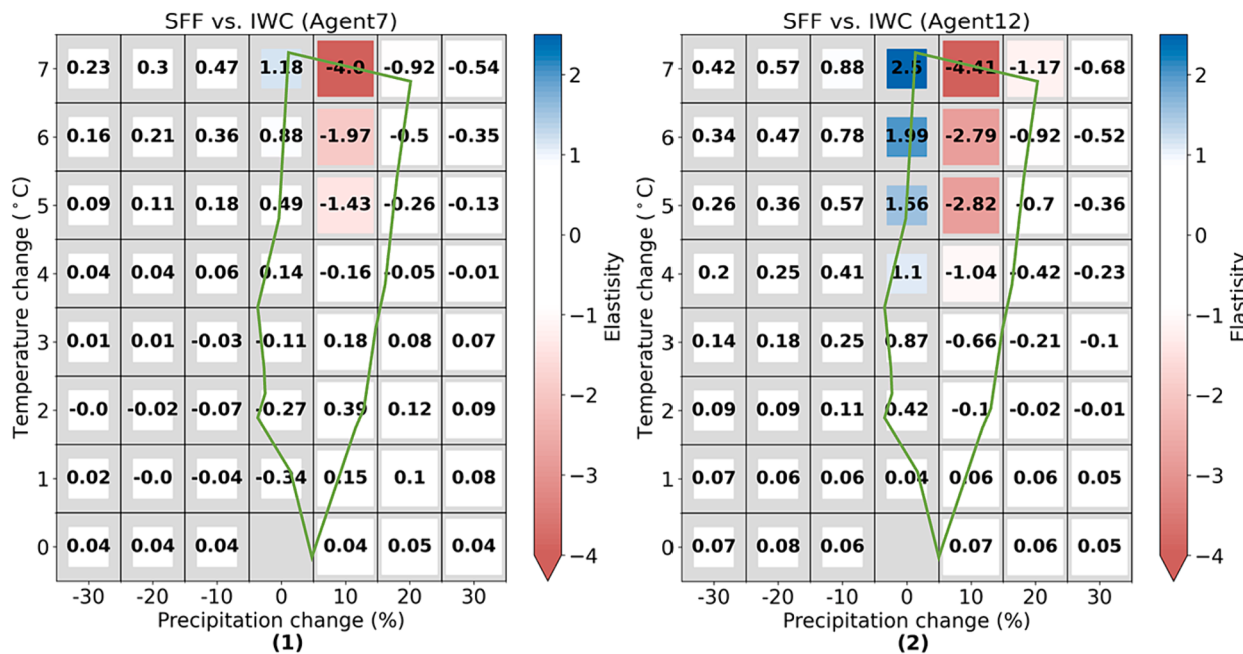


Fig. 9. Climate response surfaces for elasticity on ecosystem sector and food sector for Agent 7 and Agent 12. SFF represents the Season Flow Fraction and IWC represents Irrigated Water Consumption. The green polygon is the boundary of GCM projections to visualize the possible range of climate change. The smaller size of the colored grid indicates the average annual irrigated water consumption is lower than the baseline level. (For interpretation of the references to color in this figure legend, the reader is referred to the web version of this article.)

experience a trade-off when precipitation increases by 10 % combined with a temperature increase of 4 °C, as well as when precipitation increases by 20 % combined with a temperature increase of 7 °C.

5. Discussion

5.1. Modeling result implications for policy in CRT renegotiation

The management of the transboundary FEW nexus in the CRB is partially guided by the Columbia River Treaty (CRT), established in 1964 between Canada and the United States. The CRT regulates dam development and operation along the river, primarily for power generation and flood control and the treaty assigns rights and obligations to federal agencies in both countries. However, when the CRT was initially established, it did not explicitly consider the rights and responsibilities of tribes and residents, nor did it address critical issues such as fishing, restoration, and agricultural water use. Currently, the U.S. and Canada are renegotiating the CRT, with a focus on improving ecosystems and minimizing adverse effects on tribal resources (Congressional Research Service, 2023).

Our model delineates the interplay and trade-offs among multiple sectors across scales under differing climatic scenarios, with irrigated water consumption being pivotal. Gantla et al. (2015) indicated that people in the Pacific Northwest are generally aware of the higher risk of food shortages and crop failures due to climate change. Additionally, Zhang et al. (2021) found that residents in the CRB showed stronger support for policies related to food and water. This public awareness presents an opportunity for policymakers to advocate for water-saving technologies, potentially reducing irrigated water consumption and its associated trade-offs. Moreover, to preserve salmon habitats in the mainstream, increasing spring and summer flows via reservoir reoperation and the development of a joint program for fish passage to mitigate associated trade-offs is suggested (Congressional Research Service, 2023). A similar recommendation has been made in the CRT renegotiation process by the U.S. Army Corps of Engineers and the Bonneville Power Administration. This could come through the expansion of agreements to further augment flows for spring and summer (with these flows coming from reduced fall and winter drafts in Canadian reservoirs) and the development of a joint program for fish passage (Congressional Research Service, 2023).

5.2. Limitations and future work

The proposed modeling framework has some limitations that need to be addressed in future studies. One of the limitations is that the current model assumes that agents' behaviors follow the Bayesian inference on water availability and simple economic optimization for agriculture production, which may not adequately capture the decision-making mechanisms of all agents. For example, crop demands, and water-saving technologies, may also be part of the considerations. Additionally, the model does not explicitly consider direct interactions among agents, such as peer pressure, water rights and water markets (Du et al., 2020). Many studies have shown the social norm effect is an essential factor influencing human behavior especially at the smaller spatial scale (Bicchieri and Muldoon, 2011; Cedeno-Mieles et al., 2020). Future research could conduct in-depth interviews or surveys with different farmers in different subbasins (agents) to advance our understanding in farmers' empirical decision-making processes in specific locations and investigate how these farmers make decisions in the face of uncertainties in crop price, water resources fee and water availability. Another limitation of the model is that it does not account for the agents' crop selection, double cropping, and crop area decisions. The model assumes that agents' irrigated water consumption reflects these factors, but in reality, warming and an extension of the growing season may result in the adoption of slower-growing crop varieties and an increase in double-cropping. Therefore, future work could include a crop selection module

in the ABM to better reflect the reality. In addition, the current model only considers irrigated water consumption and does not account for water consumption by other sectors (e.g., hydropower and municipal). To overcome this limitation, future research could enhance the current model by incorporating additional types of agents (e.g., hydropower, urban, and ecosystem), which could represent sectors such as reservoir operations, urban public water supply, and ecological water needs. This expanded framework with the direct and indirect interactions among these different types of agents would facilitate a more comprehensive and accurate future analysis of the FEW nexus under climate change. Finally, we only use CMIP5 scenarios in this study to inform future climate change likelihood. Given the flexibility of the Decision scaling method, when all CMIP6 downscaled data become available, they can also be superimposed on top of our climate response surface (e.g., Figs. 6, 8, and 9) to show the latest future climate change projection.

6. Conclusion

Growing energy and food demands, coupled with increasing uncertainties in the hydrologic cycle due to climate change, will challenge effective water resources management in the coming decades. To address this challenge, a better understanding of the co-evolution mechanism in coupled natural-human systems (CNHS) and its influence on the food, energy, water (FEW) nexus under changing climate forcing and human decisions is critical. This study developed a novel modeling framework by integrating an agent-based model (ABM) into a large-scale hydrologic model for co-evolution analysis to address the interaction between human and natural systems. The proposed integrated ABM framework characterizes human decision-making processes on irrigation by considering heterogeneous initial expectations on water availability and updating those perceptions with recent experience using Bayesian inference. Different decay rate of memory and foresight regarding external constraints on the water availability are also conceptually included in the model. Subsequently, a comprehensive analysis that spans multiple sectors and across multiple scales was conducted by utilizing the outputs from the developed integrated modeling framework, which provide valuable insights for strategic planning and sustainable resource management under varying climatic conditions. The developed framework is applied in the Columbia River Basin for demonstration, but it can be easily applied to other basins.

Calibration and validation results of the integrated model show that our methodology can potentially capture, at least partially, the historical complexities of human activities (irrigated water consumption) and natural dynamics (streamflow changes). The results of our scenario analyses indicate that under hotter and wetter climate conditions, the trade-off between irrigated water consumption, hydropower generation, and streamflow will become more pronounced at both the basin and regional levels. Specially, the trade-off is expected to increase under more extreme climate change scenarios, characterized by a temperature increase greater than 4 °C and an increase in precipitation of 10 % during the growing season. In addition, the trade-off is more sensitive to variations in temperature during the non-growing season with no precipitation change. At the regional level, the findings suggest that it will be more challenging to balance the timing of crop production and hydropower generation under climate change impacts. Furthermore, it is crucial to identify the "temperature thresholds" characteristics of distinct regions, at which the trade-off patterns begin to emerge. Lastly, region-specific water management policies will be needed to effectively address the trade-offs arising from climate change for both upstream and downstream states. Further analysis utilizing more realistic modeling frameworks is still needed to better quantify the co-evolution in informing policymaking for future multi-sector and multi-level water resources governance applications in the CNHS.

CRediT authorship contribution statement

Jiaorui Zhang: Conceptualization, Formal analysis, Methodology, Writing – original draft. **Y.C. Ethan Yang:** Conceptualization, Funding acquisition, Project administration, Supervision, Writing – review & editing. **Guta W. Abeshu:** . **Hongyi Li:** Funding acquisition, Writing – review & editing. **Fengwei Hung:** Methodology, Writing – review & editing. **Chung-Yi Lin:** Investigation, Writing – review & editing. **L. Ruby Leung:** Methodology, Supervision, Writing – review & editing.

Declaration of competing interest

The authors declare that they have no known competing financial interests or personal relationships that could have appeared to influence the work reported in this paper.

Data availability

Data will be made available on request.

Acknowledgement

This paper is supported by the US National Science Foundation (EAR #1804560). We would like to thank the editor, the associate editor, and two anonymous reviewers for their comments and suggestions to improve the quality of the manuscript. Pacific Northwest National Laboratory (PNNL) is operated for the US Department of Energy by Battelle Memorial Institute under contract DE-AC05-76RL01830.

Appendix A. Supplementary data

Supplementary data to this article can be found online at <https://doi.org/10.1016/j.jhydrol.2024.131048>.

References

- Abeshu, G.W., Tian, F., Wild, T., Zhao, M., Turner, S., Chowdhury, A.F.M.K., Vernon, C.R., Hu, H., Zhuang, Y., Hejazi, M., Li, H.-Y., 2023. Enhancing the representation of water management in global hydrological models. *Geosci. Model Dev. Discuss.* 1–41. <https://doi.org/10.5194/gmd-2023-12>.
- Alderman, P., Bost, J., Breuer, N. E., Gill, T., Graves, D., Hildebrand, P., Livengood, E., Mishkin, M., Ward, D.R. and Wilsey, D., 2007. Farming systems and farmer decision making in Columbia and Suwannee Counties. Southeast Climate Consortium Technical Report Series: SECC-07-002. Gainesville, Florida.
- Bhatt, G., Kumar, M., Duffy, C.J., 2014. A tightly coupled GIS and distributed hydrologic modeling framework. *Environ. Model. Softw.* 62, 70–84. <https://doi.org/10.1016/j.envsoft.2014.08.003>.
- Bicchieri, C., Muldoon, R., 2011. Social Norms.
- Bieber, N., Ker, J.H., Wang, X., Triantafyllidis, C., van Dam, K.H., Koppelaar, R.H.E.M., Shah, N., 2018. Sustainable planning of the energy-water-food nexus using decision making tools. *Energy Policy* 113, 584–607. <https://doi.org/10.1016/j.enpol.2017.11.037>.
- Brown, C., Ghile, Y., Laverty, M., Li, K., 2012. Decision scaling: linking bottom-up vulnerability analysis with climate projections in the water sector. *Water Resour. Res.* 48 (9).
- Castilla-Rho, J.C., Mariethoz, G., Rojas, R., Andersen, M.S., Kelly, B.F., 2015. An agent-based platform for simulating complex human-aquifer interactions in managed groundwater systems. *Environ. Model. Softw.* 73, 305–323. <https://doi.org/10.1016/j.envsoft.2015.08.018>.
- Cedeno-Mieles, V., Hu, Z., Ren, Y., Deng, X., Adiga, A., Barrett, C., et al., 2020. Networked experiments and modeling for producing collective identity in a group of human subjects using an iterative abduction framework. *Soc. Netw. Anal. Min.* 10 (1), 1–43.
- Chang, H., Psaris, M., 2013. Local landscape predictors of maximum stream temperature and thermal sensitivity in the Columbia River basin, USA. *Sci. Total Environ.* 461, 587–600.
- Chegwidden, O.S., Rupp, D.E., Nijssen, B., 2020. Climate change alters flood magnitudes and mechanisms in climatically-diverse headwaters across the northwestern United States. *Environ. Res. Lett.* 15 (9), 094048.
- Cole, V.T., Bauer, D.J., 2016. A note on the use of mixture models for individual prediction. *Structural Equation Modeling: A Multidisciplinary Journal* 23 (4), 615–631.
- Columbia River Inter-Tribal Fish Commission, 2013. Salmon Culture. <http://www.critfc.org/salmon-culture/tribal-salmon-culture>. (Accessed 27 January 2023).
- Congressional Research Service, 2023. Columbia River Treaty Review. <https://sgp.fas.org/crs/misc/R43287.pdf>. (Accessed 20 February 2023).
- Crozier, L., 2015. Impacts of climate change on salmon of the Pacific Northwest. Seattle.
- Dalton, M., Mote, P.W., Snover, A.K., 2013. Climate change in the northwest: implications for our landscapes, waters, and communities. Island Press, Washington, D.C., p. 271
- Du, E., Tian, Y., Cai, X., Zheng, Y., Li, X., Zheng, C., 2020. Exploring spatial heterogeneity and temporal dynamics of human-hydrological interactions in large river basins with intensive agriculture: a tightly coupled, fully integrated modeling approach. *J. Hydrol.* 591, 125313 <https://doi.org/10.1016/j.jhydrol.2020.125313>.
- Eisele, M., Troost, C., Berger, T., 2021. How bayesian are farmers when making climate adaptation decisions? a computer laboratory experiment for parameterising models of expectation formation. *J. Agric. Econ.* 72 (3), 805–828.
- English, M.J., Solomon, K.H., Hoffman, G.J., 2002. A paradigm shift in irrigation management. *J. Irrig. Drain. Eng.* 128 (5), 267–277.
- Featherstone, A.M., Moghnieh, G.A., Goodwin, B.K., 1995. Farm-level nonparametric analysis of cost-minimization and profit-maximization behavior. *Agric. Econ.* 13 (2), 109–117.
- Foran, T., 2015. Node and regime: interdisciplinary analysis of water-energy-food nexus in the Mekong region. *Water Altern.* 8 (1).
- Gaddam, S.J., Sampath, P.V., 2022. Are multiscale water-energy-land-food nexus studies effective in assessing agricultural sustainability? *Environ. Res. Lett.* 17 (1), 014034.
- Gadgil, S., Rao, P.S., Rao, K.N., 2002. Use of climate information for farm-level decision making: rainfed groundnut in southern India. *Agr. Syst.* 74 (3), 431–457.
- Gantla, S., L. Bernacchi, J. D. Wulfhorst, M. Reyna, L. N. McNamee, S. Irizarry, S. Kane, and B. Foltz. 2015. "Climate change risk perceptions and adaptive strategies among Inland Pacific Northwest wheat producers, regional approaches to climate change." https://www.reacchpna.org/sites/files/Climate_Change_and_Associated_Risk_Perceptions_3-4-15.pdf. (Accessed 14 July 2021).
- Giuliani, M., Li, Y., Castelletti, A., Gandolfi, C., 2016. The coupled human-natural systems analysis of irrigated agriculture under changing climate. *J. Am. Water Resour. Assoc.* 52, 6928–6947. <https://doi.org/10.1002/2016WR019363>.
- Gupta, H.V., Kling, H., Yilmaz, K.K., Martinez, G.F., 2009. Decomposition of the mean squared error and NSE performance criteria: implications for improving hydrological modelling. *J. Hydrol.* 377 (1–2), 80–91. <https://doi.org/10.1016/j.jhydrol.2009.08.003>.
- Hamlet, A.F., Lettenmaier, D.P., 1999. Effects of climate change on hydrology and water resources in the Columbia River basin. *J. Am. Water Resour. Assoc.* 35 (6), 1597–1623.
- Harrell, J., Nijssen, B., Frans, C., 2022. Where and when does streamflow regulation significantly affect climate change outcomes in the Columbia River basin? *Water Resour. Res.* 58 (10), e2022WR031950.
- Holdschlag, A., Ratter, B.M., 2013. Multiscale system dynamics of humans and nature in the Bahamas: perturbation, knowledge, panarchy and resilience. *Sustain. Sci.* 8, 407–421.
- Holtz, G., Pahl-Wostl, C., 2012. An agent-based model of groundwater over-exploitation in the upper guadiana, Spain. *Reg. Environ. Chang.* 12, 95–121. <https://doi.org/10.1007/s10113-011-0238-5>.
- Hu, Y., Cai, X., DuPont, B., 2015. Design of a web-based application of the coupled multi-agent system model and environmental model for watershed management analysis using hadoop. *Environ. Model. Softw.* 70, 149–162. <https://doi.org/10.1016/j.envsoft.2015.04.011>.
- Huang, Z., Hejazi, M., Li, X., Tang, Q., Vernon, C., Leng, G., Wada, Y., 2018. Reconstruction of global gridded monthly sectoral water withdrawals for 1971–2010 and analysis of their spatiotemporal patterns. *Hydrol. Earth Syst. Sci.* 22 (4), 2117–2133.
- Hung, F., Son, K., Yang, Y.E., 2022. Investigating uncertainties in human adaptation and their impacts on water scarcity in the Colorado river basin, United States. *J. Hydrol.* 612, 128015.
- Independent Scientific Group, 2000. Return to the river: restoration of salmonid fishes in the Columbia River ecosystem. Report to the Northwest. Power and Conservation Council. <http://www.nwcouncil.org/reports/2000/2000-12>. (Accessed 13 March 2021).
- Kahil, T., Parkinson, S., Satoh, Y., Greve, P., Burek, P., Veldkamp, T.I., Wada, Y., 2018. A continental-scale hydroeconomic model for integrating water-energy-land nexus solutions. *Water Resour. Res.* 54 (10), 7511–7533.
- Khalvati, K., Park, S.A., Mirbagheri, S., Philippe, R., Sestito, M., Dreher, J.C., Rao, R.P., 2019. Modeling other minds: bayesian inference explains human choices in group decision-making. *Sci. Adv.* 5 (11), eaax8783.
- Khan, H.F., Yang, Y.C.E., Xie, H., Ringler, C., 2017. A coupled modeling framework for sustainable watershed management in transboundary river basins. *Hydrol. Earth Syst. Sci.* 21 (12), 6275–6288. <https://doi.org/10.5194/hess-21-6275-2017>.
- Khanal, R., Brady, M.P., Stöckle, C.O., Rajagopalan, K., Yoder, J., Barber, M.E., 2021. The economic and environmental benefits of partial leasing of agricultural water rights. *Water Resour. Res.* 57, e2021WR029712 <https://doi.org/10.1029/2021WR029712>.
- Kling, H., Fuchs, M., Paulin, M., 2012. Runoff conditions in the upper Danube basin under an ensemble of climate change scenarios. *J. Hydrol.* 424, 264–277.
- Kluger, L.C., Gorris, P., Kochalski, S., Mueller, M.S., Romagnoni, G., 2020. Studying human–nature relationships through a network lens: a systematic review. *People and Nature* 2 (4), 1100–1116. <https://doi.org/10.1002/pan3.10136>.
- Kraucunas, I., Clarke, L., Dirks, J., et al., 2015. Investigating the nexus of climate, energy, water, and land at decision-relevant scales: the platform for regional integrated modeling and analysis (PRIMA). *Clim. Change* 129, 573–588. <https://doi.org/10.1007/s10584-014-1064-9>.

- Leck, H., Conway, D., Bradshaw, M., Rees, J., 2015. Tracing the water–energy–food nexus: description, theory and practice. *Geogr. Compass* 9 (8), 445–460. <https://doi.org/10.1111/gec3.12222>.
- Lehner, B., Liermann, C.R., Revenga, C., Vörösmarty, C., Fekete, B., Crouzet, P., Wisser, D., 2011. High-resolution mapping of the world's reservoirs and dams for sustainable river-flow management. *Front. Ecol. Environ.* 9 (9), 494–502.
- Lei, X., Zhao, J., Yang, Y.-C.-E., Wang, Z., 2019. Comparing the economic and environmental effects of different water management schemes using a coupled agent-hydrologic model. *J. Water Resour. Plan. Manag.* 145 (6), 05019010. [https://doi.org/10.1061/\(ASCE\)WR.1943-5452.0001074](https://doi.org/10.1061/(ASCE)WR.1943-5452.0001074).
- Li, X., Vernon, C.R., Hejazi, M.I., Link, R.P., Feng, L., Liu, Y., Rauchenstein, L.T., 2017. Xanthos—a global hydrologic model. *Journal of Open Research Software* 5 (PNL-SA-126584).
- Lin, C.Y., Yang, Y.E., Malek, K., Adam, J.C., 2022. An exploration of interconnected natural and human systems using a bi-directional agent-based modeling framework. *Environ. Model. Softw.* 155, 105451.
- Liu, Y., Hejazi, M., Li, H., Zhang, X., Leng, G., 2018. A hydrological emulator for global applications—HE v1. 0.0. *Geosci. Model Dev.* 11 (3), 1077–1092.
- Liu, J., Mooney, H., Hull, V., Davis, S.J., Gaskell, J., Hertel, T., Lubchenco, J., Seto, K.C., Gleick, P., Kremen, C., Li, S., 2015. Systems integration for global sustainability. *Science* 347 (6225), 1258832.
- Lizumi, T., Ramankutty, N., 2015. How do weather and climate influence cropping area and intensity? *Glob. Food Sec.* 4, 46–50.
- Luce, C.H., Lopez-Burgos, V., Holden, Z., 2014. Sensitivity of snowpack storage to precipitation and temperature using spatial and temporal analog models. *Water Resour. Res.* 50 (12), 9447–9462.
- Magliocca, N.R., 2020. Agent-based modeling for integrating human behavior into the food–energy–water nexus. *Land* 9 (12), 519.
- Mantua, N., Tohver, I., Hamlet, A., 2010. Climate change impacts on streamflow extremes and summertime stream temperature and their possible consequences for freshwater salmon habitat in Washington State. *Clim. Change* 102 (1–2), 187–223.
- Motesharrei, S., Rivas, J., Kalnay, E., 2014. Human and nature dynamics (HANDY): modeling inequality and use of resources in the collapse or sustainability of societies. *Ecol. Econ.* 101, 90–102.
- Moyo, M., Mvumi, B.M., Kunzweguta, M., Mazvimavi, K., Craufurd, P., Dorward, P., 2012. Farmer perceptions on climate change and variability in semi-arid Zimbabwe in relation to climatology evidence. *Afr. Crop Sci. J.* 20, 317–335.
- Müller, B., Bohn, F., Dreßler, G., Groeneveld, J., Klassert, C., Martin, R., et al., 2013. Describing human decisions in agent-based models—ODD+ D, an extension of the ODD protocol. *Environ. Model. Softw.* 48, 37–48.
- Nawab, A., Liu, G., Meng, F., Hao, Y., Zhang, Y., 2019. Urban energy-water nexus: spatial and inter-sectoral analysis in a multi-scale economy. *Ecol. Model.* 403, 44–56.
- Newell, J.P., Goldstein, B., Foster, A., 2019. A 40-year review of food–energy–water nexus literature and its application to the urban scale. *Environ. Res. Lett.* 14 (7), 073003.
- Ng, T.L., Eheart, J.W., Cai, X., Braden, J.B., 2011. An agent-based model of farmer decision-making and water quality impacts at the watershed scale under markets for carbon allowances and a second generation biofuel crop. *Water Resour. Res.* 47 (9), W09519. <https://doi.org/10.1029/2011WR010399>.
- Nicenboim, B., Schad, D., & Vasishth, S., 2021. An introduction to Bayesian data analysis for cognitive science. Under contract with Chapman and Hall/CRC statistics in the social and behavioral sciences series.
- NPCC, 2005. Subbasin Plans. <https://www.nwcouncil.org/subbasin-plans>. (Accessed 30 May 2019).
- O'Hagan, A., 1998. Eliciting expert beliefs in substantial practical applications. *Journal of the Royal Statistical Society Series d: the Statistician* 47 (1), 21–35.
- Olarinde, L.O., Manyong, V.M., Okoruwa, V.O., 2008. Analysing optimum and alternative farm plans for risk averse grain crop farmers in Kaduna state, northern Nigeria. *World Journal of Agricultural Sciences* 4 (1), 28–35.
- Payne, J.T., Wood, A.W., Hamlet, A.F., Palmer, R.N., Lettenmaier, D.P., 2004. Mitigating the effects of climate change on the water resources of the Columbia River basin. *Clim. Change* 62, 233–256.
- Press, S.J., 2002. Subjective and objective bayesian statistics, principles, models and applications, 2nd edition. John Wiley and Sons Inc, N. J.
- Rajagopalan, K., Chinnayakanahalli, K.J., Stockle, C.O., Nelson, R.L., Kruger, C.E., Brady, M.P., et al., 2018. Impacts of near-term climate change on irrigation demands and crop yields in the Columbia River basin. *Water Resour. Res.* 54, 2152–2182. <https://doi.org/10.1002/2017WR020954>.
- Reed, P.M., Hadjimichael, A., Moss, R.H., Breisford, C., Burleyson, C.D., Cohen, S., et al., 2022. Multisector dynamics: advancing the science of complex adaptive human-earth systems. *Earth's Future*, 10 (3), e2021EF002621. <https://doi.org/10.1029/2021EF002621>.
- Salimonu, K.K., Falusi, A.O., 2007. Risk preferences and resource allocation differentials of food crop farmers. *Journal of Rural Economics and Development* 16 (1623–2016-134882), 1–12.
- Sankarasubramanian, A., Vogel, R.M., 2003. Hydroclimatology of the continental United States. *Geophys. Res. Lett.* 30 (7).
- Sankarasubramanian, A., Vogel, R.M., Limbrunner, J.F., 2001. Climate elasticity of streamflow in the United States. *Water Resour. Res.* 37 (6), 1771–1781.
- Sauter, S.T., McMillan, J., Dunham, J.B., 2001. Salmonid behavior and water temperature. Seattle, WA: United States, Environmental Protection Agency, region 10 Office of Water. final report to the policy workgroup of the EPA region 10 water temperature criteria guidance project. EPA 910-D-01-001, 36 p.
- From Climate to Flow, in *Climate Change and u.s. Water Resources* 8, 1990, 177–206.
- Siddiqi, A., Kajenthira, A., Anadón, L.D., 2013. Bridging decision networks for integrated water and energy planning. *Energ. Strat. Rev.* 2 (1), 46–58. <https://doi.org/10.1016/j.est.2013.02.003>.
- Siderius, C., Conway, D., Yassine, M., Murken, L., Losti, P.L., Dalin, C., 2020. Multi-scale analysis of the water-energy-food nexus in the Gulf region. *Environ. Res. Lett.* 15 (9), 094024.
- Sivapalan, M., Blöschl, G., 2015. Time scale interactions and the co-evolution of humans and water. *Water Resour. Res.* 51 (9), 6988–7022.
- Stewart, I.T., Cayon, D.R., Dettinger, M.D., 2005. Changes toward earlier streamflow timing across western North America. *J. Clim.* 18 (8), 1136–1155.
- Tesfatsion, L., 2017. Modeling economic systems as locally-constructive sequential games. *J. Econ. Methodol.* 24 (4), 384–409.
- Thomas, H., 1981. Improved methods for national water assessment, report WR15249270. US Water Resource Council, Washington, DC.
- U.S. Energy Information Administration, 2014. The Columbia River Basin provides more than 40% of total U.S. hydroelectric generation. <https://www.eia.gov/todayinenergy/detail.php?id=16891#>. (Accessed 16 March 2023).
- Van Vuuren, D.P., Edmonds, J., Kainuma, M., Riahi, K., Thomson, A., Hibbard, K., Rose, S.K., 2011. The representative concentration pathways: an overview. *Clim. Change* 109, 5–31.
- Vernon, C.R., Hejazi, M.I., Turner, S.W., Liu, Y., Braun, C.J., Li, X., Link, R.P., 2019. A global hydrologic framework to accelerate scientific discovery. *Journal of Open Research Software* 7 (1), 1.
- Vogt, C., Zimmermann, M., Brekke, K., 2014. Operationalizing the urban nexus: towards resource-efficient and integrated cities and metropolitan regions. Deutsche Gesellschaft für Internationale Zusammenarbeit GmbH, Eschborn.
- Voisin, N., Liu, L., Hejazi, M., Tesfa, T., Li, H., Huang, M., Leung, L.R., 2013. One-way coupling of an integrated assessment model and a water resources model: evaluation and implications of future changes over the US Midwest. *Hydrol. Earth Syst. Sci.* 17 (11), 4555–4575.
- Wada, Y., Wisser, D., Bierkens, M.F., 2014. Global modeling of withdrawal, allocation and consumptive use of surface water and groundwater resources. *Earth Syst. Dyn.* 5 (1), 15–40.
- Weedon, G.P., Gomes, S., Viterbo, P., Shuttleworth, W.J., Blyth, E., ÖSterle, H., Adam, J. C., Bellouin, N., Boucher, O., Best, M., 2011. Creation of the WATCH forcing data and its use to assess global and regional reference crop evaporation over land during the twentieth century. *J. Hydrometeorol.* 12 (5), 823–848. <https://doi.org/10.1175/2011JHM1369.1>.
- Williams, T., & Hardison, P., 2006. Impacts on Indigenous peoples. Parker, A., et al Climate Change and Pacific Rim Indigenous Nations. Olympia, WA: Northwest Indian Applied Research Center, The Evergreen State College.
- Yang, Y.E., Son, K., Hung, F., Tidwell, V., 2020. Impact of climate change on adaptive management decisions in the face of water scarcity. *J. Hydrol.* 588, 125015.
- Yoon, J., Romero-Lankao, P., Yang, Y.E., Klassert, C., Urban, N., Kaiser, K., Keller, K., Yarlagadda, B., Voisin, N., Reed, P.M., Moss, R., 2022. A typology for characterizing human action in multisector dynamics models. *earth's Future* 10 (8), e2021EF002641.
- Zhang, J., Yang, Y.C.E., Li, H., Shittu, E., 2021. Examining the food-energy-water-environment nexus in transboundary river basins through a human dimension lens: Columbia River basin. *J. Water Resour. Plan. Manag.* 147 (10), 05021019.
- Zhou, Y., Hejazi, M., Smith, S., Edmonds, J., Li, H., Clarke, L., Calvin, K., Thomson, A., 2015. A comprehensive view of global potential for hydro-generated electricity. *Energ. Environ. Sci.* 8 (9), 2622–2633. <https://doi.org/10.1039/C5EE00888C>.